Biological Conservation 319 (2026) 111900

Contents lists available at ScienceDirect

Biological Conservation

journal homepage: www.elsevier.com/locate/biocon

Disturbance and incomplete recovery in the Cerrado-Amazon transition: Implications for conservation of a critical tropical ecotone

Chuanze Li [a,*], Angela Harris [a], Beatriz Schwantes Marimon [b], Ben Hur Marimon Junior [b], Matthew Dennis [a], Ricardo Dalagnol [c], Polyanna da Conceição Bispo [a]

[a] Department of Geography, School of Environment, Education and Development, University of Manchester, Oxford Road, Manchester, M13 9PL, UK
[b] Universidade do Estado de Mato Grosso, Campus de Nova Xavantina, Nova Xavantina, MT, 78690-000, Brazil
[c] CTREES, Pasadena, 91105, CA, USA

ARTICLE INFO

Keywords:
Cerrado-Amazon Transition (CAT)
Disturbance hotspots
Landsat time series
LandTrendr
Vegetation disturbance
Clear-cutting and fire

ABSTRACT

The Cerrado-Amazon Transition (CAT) is the world's largest tropical forest–savanna ecotone and a key component of Brazil's "Arc of Deforestation". It harbours high biodiversity but remains weakly protected and increasingly exposed to agricultural expansion, deforestation, and fire. Using Landsat time series (1986–2020), we developed a disturbance–recovery framework to track how repeated and interacting disturbances reshape vegetation dynamics across the CAT. By combining LandTrendr to reconstruct disturbance histories, a residual neural network to distinguish disturbance pathways, and NBR-based proxy indicators to quantify disturbance-related spectral losses and post-disturbance trajectories, the framework captures both compound disturbance patterns and signals of resilience erosion. We identified four major disturbance trajectories associated with clear-cutting and fire. Over the past 35 years, approximately 493,000 km^2 of the CAT experienced at least one disturbance event, with clear-cutting dominating in Amazon forest and recurrent fire affecting both Amazon forest and Cerrado vegetation. Disturbance hotspots were concentrated near farming and ranching landscapes, while large areas of repeatedly disturbed vegetation remained outside the current protected-area network. Most fire-affected trajectories in both Amazon forest and Cerrado did not fully recover within 10 years, indicating persistent post-disturbance spectral legacies; although proxy indicator captures spectral recovery rather than all dimensions of ecosystem recovery, this pattern is consistent with widespread erosion of vegetation resilience under repeated disturbance pressure. By identifying hotspots of recurrent disturbance and incomplete recovery, and revealing major protection gaps, this study provides a practical basis for conservation planning, enforcement, and restoration across high-pressure frontier landscapes.

1. Introduction

The Cerrado-Amazon Transition (CAT) zone is the Earth's largest tropical ecotone, forming the boundary between Brazil's Cerrado savanna and the Amazon rainforest biomes (Marques et al., 2020). Spanning ~6000 km, the CAT hosts a diverse array of plant species and structural formations (Marques et al., 2020; Projeto RADAMBRASIL, 1981) and encompasses transitional vegetation types from both biomes. This ecological diversity contributes to dynamic boundaries and strong spatial heterogeneity in vegetation structure (de Souza Mendes et al., 2019; Marques et al., 2020; Ratter et al., 1973; Torello-Raventos et al., 2013). The CAT ecotone also plays a disproportionate role in maintaining habitat continuity, carbon stocks and regional water and energy fluxes, but remains weakly protected compared with the Amazon core region. As a result, it has become a conservation priority in discussions about protected-area expansion, ecological corridors, and climate mitigation in tropical South America. Despite its ecological significance, however, the CAT is subject to intense anthropogenic and natural pressures, particularly deforestation and fire.

Driven largely by the expansion of agriculture and pasturelands, clear-cutting has become one of the most pervasive disturbances in the CAT (Flores et al., 2024; Ribeiro et al., 2024). This process triggers cascading ecological consequences, including vegetation carbon loss, biodiversity decline and soil degradation (Almeida et al., 2018; Bonini et al., 2018; Coe et al., 2013; Maia et al., 2010; Wearn et al., 2012). Fire activity has also been widespread across the CAT over the past four

* Corresponding author at: Flat1119, 6 Nobel Way, Manchester, M1 7FH, UK.
E-mail address: chuanze.li@postgrad.manchester.ac.uk (C. Li).

https://doi.org/10.1016/j.biocon.2026.111900
Received 18 December 2025; Received in revised form 30 April 2026; Accepted 8 May 2026
Available online 14 May 2026

decades (Ribeiro et al., 2024), primarily associated with human-driven land clearing and management and the conversion of land for agriculture and cattle ranching (Cerri et al., 2018; Fearnside, 2005; Matricardi et al., 2013). Such disturbance regimes not only alter vegetation structure and productivity, but also threaten biodiversity, increase the risk of shifts to degraded vegetation states, and undermine key ecosystem services such as carbon storage and regional climate regulation. Although previous studies have documented disturbance in specific sites or sub-regions (Marques et al., 2024; Reygadas et al., 2021; de Souza et al., 2021), a cross-CAT understanding of disturbance timing, frequency, and spatial patterns remains limited because of the region's ecological heterogeneity and spatial complexity.

Understanding how vegetation recovers after disturbance is essential for assessing ecosystem resilience, estimating carbon fluxes, and guiding long-term land management and conservation strategies. Incomplete or slow recovery can lead to sustained carbon emissions, shifts in biome boundaries, and feedbacks that disrupt regional hydrology and climate (Aragão et al., 2018; Pellegrini et al., 2018; Silva Junior et al., 2020). Recovery capacity can vary markedly across vegetation types and ecological settings. For example, seasonally dry forests in the CAT may be more fire-resilient because they contain fire-adapted species and often have lower fuel loads (Balch et al., 2011; Hoffmann et al., 2012; Ribeiro and Walter, 2008). In contrast, seasonally flooded Amazonian forests can become highly fire-sensitive during droughts. Under dry conditions, their moisture-rich root systems may dry out and become more flammable (Maracahipes et al., 2014). However, because recovery has not been assessed across the full extent of the CAT, the extent to which these contrasting recovery patterns apply to the region remains poorly understood.

Previous studies have provided important insights into disturbance and recovery near the Amazon–Cerrado boundary, but key limitations remain for understanding the CAT as a whole. Fire occurrence and clear-cutting have been documented in specific sites or sub-regions (Marques et al., 2024; Reygadas et al., 2021; de Souza et al., 2021), yet a consistent CAT-wide assessment of disturbance timing, frequency, and spatial patterns is still lacking. In addition, many studies focus on disturbance occurrence or land-cover change at specific time points (de Souza Mendes et al., 2019; Morton et al., 2006; Wang et al., 2019; Zaiatz et al., 2018), which may overlook disturbance signals that do not translate into land-cover change and cannot resolve how disturbances accumulate and interact over time. Recovery evidence within the CAT is also limited: existing studies rely mainly on field plots or coarse-resolution observations in parts of the region (Reis et al., 2015, 2017; Santana et al., 2020), and thus cannot characterise recovery trajectories across the CAT's full ecological gradients. Although post-disturbance recovery has been widely studied in the Amazon or Cerrado biomes individually (Bullock and Woodcock, 2021; Drüke et al., 2023; Machida et al., 2021; Silva et al., 2018), these findings cannot be directly extrapolated to the ecotone because of its ecological heterogeneity and transitional nature. As a result, there is still no spatially explicit, long-term framework for jointly assessing disturbance occurrence, disturbance-type differentiation, and post-disturbance trajectories across the CAT, which limits robust ecological assessment in this heterogeneous ecotone.

Earth observation (EO) data provide unique opportunities for large-scale, long-term monitoring of vegetation dynamics (Wang et al., 2019). Whilst spectral data are proxies rather than direct measurements of ecosystem attributes, they can effectively track change in vegetation condition, including shifts in canopy structure, vegetation cover, and disturbance legacies. Consequently, time series change detection algorithms applied to EO image stacks, such as LandTrendr (Kennedy et al., 2010), have been widely used to detect vegetation disturbance events and recovery patterns across diverse regions (Almeida de Souza et al., 2020; Kennedy et al., 2010; Reygadas et al., 2021; Yin et al., 2022). As such, EO time-series analysis provide a scalable and well-suited approach for characterising disturbance and post-disturbance recovery across large spatial extents (Hislop et al., 2018; Pérez-Cabello et al., 2021; Senf et al., 2019; White et al., 2018).

However, whilst conventional time series change detection methods are effective at identifying the occurrence, timing and magnitude of change a significant knowledge gap remains in our ability to automatically differentiate between specific mechanisms of disturbance. For instance, although segmentation algorithms like LandTrendr provide a robust, physically interpretable history of temporal changes, they often lack the semantic depth to distinguish between similar spectral breakpoints that may arise from fundamentally different disturbance processes or vegetation contexts (Rodman et al., 2021). This ambiguity is particularly acute in the CAT, where strong spatial heterogeneity in vegetation structure complicates the interpretation of disturbance signals and post-disturbance trajectories (de Souza Mendes et al., 2019). Disentangling disturbance mechanisms in such settings is essential for understanding ecosystem resilience and informing targeted conservation and restoration strategies.

Integrating time-series change detection with data-driven disturbance attribution offers a promising pathway to address such a challenge. Specifically, the integration of deep learning models with LandTrendr-derived trajectories offers a novel pathway for more nuanced characterisation of vegetation disturbance. By training deep-learning models on the complex, structured temporal features provided by LandTrendr, it becomes possible to move beyond simple change detection and toward automated disturbance attribution. Such an approach allows us to bridge the gap between observing an event and understanding its cause, and provides the semantically rich data required to support robust analyses of disturbance and recovery dynamics in heterogeneous tropical landscapes (Perbet et al., 2024).

In this study, we develop a new integrated, spatially explicit approach that combines Landsat time series, the LandTrendr disturbance detection algorithm and a one-dimensional residual neural network to characterise the multi-decadal disturbance regimes (fire and clear-cutting of vegetation) and post-disturbance trajectories across the CAT. Specifically, we aim to (i) understand where and when different disturbance types occurred across the CAT over the past 35 years (1986–2020), (ii) identify conservation-relevant hotspots of recurrent disturbance, and (iii) quantify differences in post-disturbance recovery between Amazon forest and Cerrado vegetation. By distinguishing disturbance pathways and recovery trajectories across vegetation contexts, this approach provides explicit evidence to support conservation planning (identifying areas of persistent disturbance pressure), fire management (identifying fire & clear-cutting compound disturbance patterns), and restoration prioritisation (highlighting disturbance types with weaker recovery) in this critical tropical ecotone.

2. Material and methods

2.1. Study area

The study area encompasses a total of 1,145,247 km^2, stretching from the southwest to the northeast along the transitional belt between the Cerrado and Amazon biomes (IBGE, 2019; Fig. 1). Given the absence of an officially recognised boundary for the CAT, we delineated the study extent based on the distribution of existing vegetation survey plots from the Plant Ecology Laboratory of the Universidade do Estado de Mato Grosso, which have been widely used to investigate vegetation dynamics in the CAT (De Faria et al., 2024; Lenza et al., 2015; Marimon et al., 2014; Marques et al., 2020; Reis et al., 2015). Specifically, we first generated a preliminary extent in ArcGIS Pro using the Minimum Bounding Geometry tool, and then extended it along the traditional Amazon–Cerrado boundary direction following previous CAT delineation studies (Marques et al., 2020), to ensure coverage of the transition belt. This procedure produced a consistent analysis domain that captures a broad and representative forest–savanna transition gradient across the ecotone. The region's climate is primarily classified as Tropical Savanna with a dry winter (Aw) and Tropical Monsoon (Am)

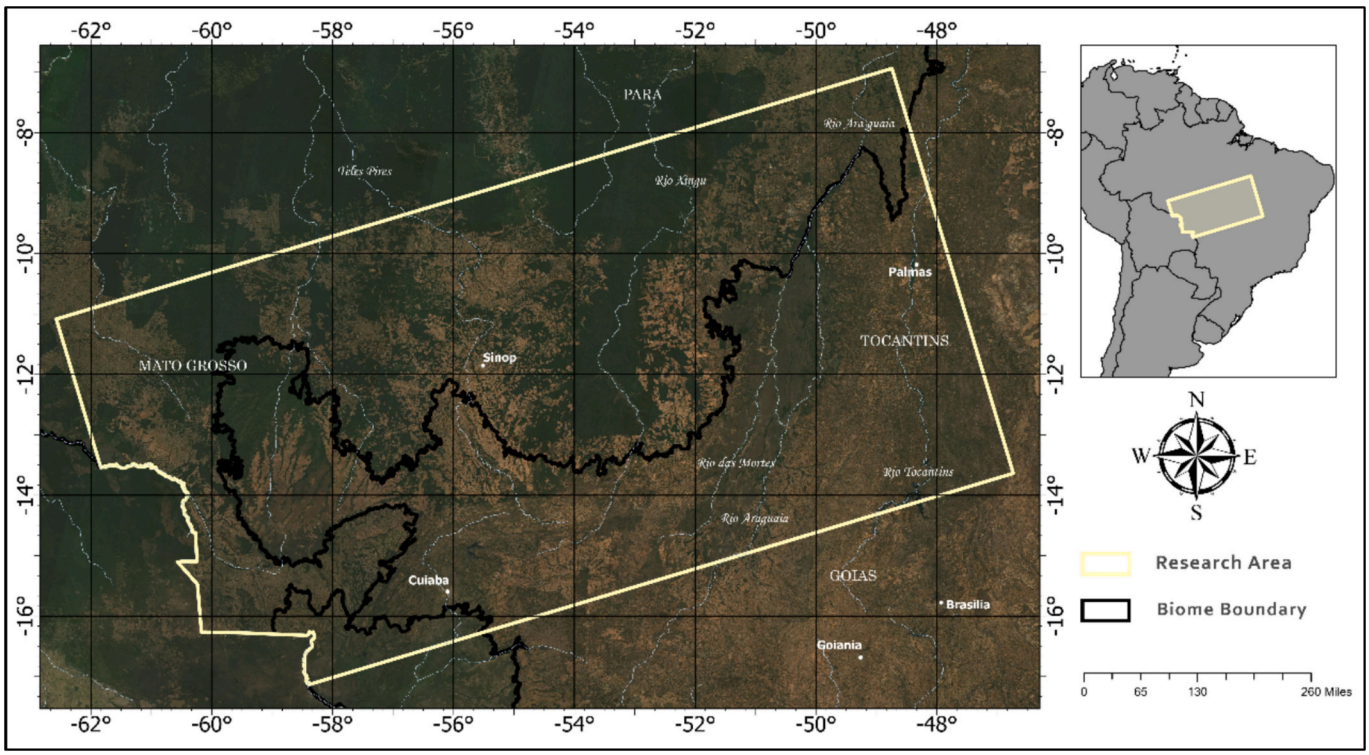

Fig. 1. The location of the CAT, encompassing part of the Brazilian States of Mato Grosso, Pará, Tocantins and Goiás. The yellow border depicts the research area; the black border is the traditional dividing line of biomes in Brazil with the Amazon biome to the north, the Cerrado biome to the south and the Pantanal at the southwest corner, near Cuiabá (IBGE, 2019). The background image is a composite of cloud-free Landsat 8 OLI scenes acquired between Jan 1 and Dec 30, 2021. (For interpretation of the references to colour in this figure legend, the reader is referred to the web version of this article.)

according to the Köppen classification system. The average annual temperature ranges from 24.1 °C to 27.3 °C, with localized dry-season temperatures reaching up to 45 °C (Araújo et al., 2021; Reis et al., 2018).

Based on the ecological heterogeneity found within the CAT, we grouped the vegetation types used in this study into two major categories; namely Amazon forest and Cerrado, with each encompassing several structurally distinct vegetation subtypes (Table 1).

Table 1
Classification and structural characteristics of Amazon forest and Cerrado within the CAT.

Categories	Description	References
Amazon Forest	Includes open ombrophilous forests, seasonal forests, gallery forests, and dry forests, primarily distributed north of the traditional biome boundary. These forests are generally more continuous and closed-canopy, with taller trees and higher biomass than Cerrado.	(Marimon et al., 2006, 2014; Ratter et al., 1973)
Cerrado	Mainly located south of the traditional biome boundary, the Cerrado comprises a gradient of vegetation types: – Cerradão (woodland savanna): Trees 8–15 m tall, canopy cover 50%–90%, featuring a mix of Amazon and Cerrado species, typically in contact zones between dry forests and other Cerrado vegetation. – Dense Cerrado: Trees 5–8 m tall, canopy cover 50%–70% – Typical Cerrado: Trees 3–6 m tall, canopy cover 20%–50% – Open Cerrado: Trees 2–3 m tall, canopy cover 5%–20%	Gonçalves et al., 2021; Marimon et al., 2014; Marimon Junior and Haridasan, 2005; Marques et al., 2020; de Oliveira et al., 2017; Ratter et al., 1973

2.2. Methods

Fig. 2 presents an overview of the methodological approach employed to identify and understand the dynamics of disturbances in the CAT from 1986 to 2020. The CAT is a highly heterogeneous ecotonal landscape in which Amazon forest and Cerrado differ in background spectral properties, seasonality, and recovery trajectories. In this setting, disturbance-type mapping is prone to confounding background variability with disturbance signals, which can reduce classification stability and interpretability. We therefore adopted a two-stage framework to separate event identification from disturbance-type differentiation, improving interpretability and reducing labelled-sample requirements for classification.

Specifically, the workflow was designed as a layered analytical chain linking (i) disturbance detection, (ii) disturbance-type differentiation, (iii) spectrally derived disturbance–recovery metrics, and (iv) resilience-oriented interpretation. In this study, we define resilience as the capacity to recover after disturbance (the degree and persistence of recovery over time). While this definition aligns most closely with an engineering-resilience perspective, it provides the necessary empirical baseline to assess ecological resilience under repeated disturbance (Gunderson, 2000; Holling, 1973). Within this context, a persistently incomplete spectral return to pre-disturbance levels indicates a recovery debt (Moreno-Mateos et al., 2017). This metric offers a spatially explicit and temporally consistent basis for comparing vegetation recovery across the CAT's diverse disturbance histories and vegetation contexts.

We first identified disturbance events using Landsat annual composite imagery and the LandTrendr disturbance detection algorithm within Google Earth Engine (GEE; Gorelick et al., 2017; Fig. 2a), which established the temporal basis (occurrence and timing) for all subsequent analyses. For each detected event, we then extracted temporal

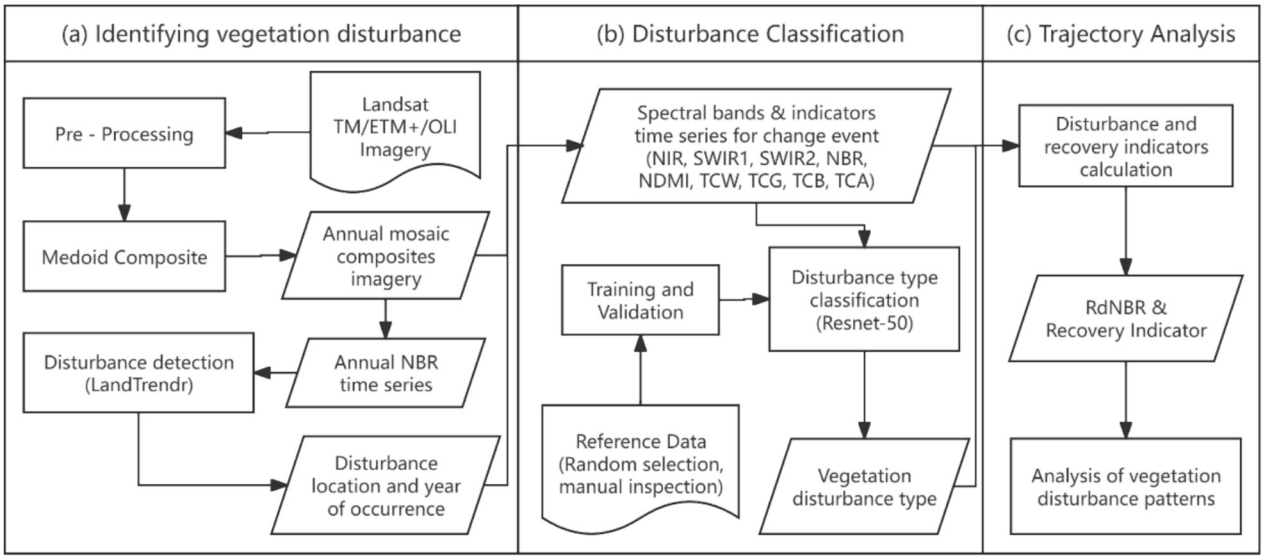

Fig. 2. Overall research approach. Abbreviations and their meaning are described in Table 4.

trajectories of Landsat spectral bands and derived spectral indices, and used these trajectories as input to a one-dimensional residual network model (1D ResNet; He et al., 2016) to classify disturbance type into four categories: (i) Amazon forest clear-cutting, (ii) Amazon forest fire, (iii) Cerrado clear-cutting, and (iv) Cerrado fire (Fig. 2b), thereby distinguishing both vegetation context and disturbance pathway. We then constructed category-specific disturbance–recovery trajectories from normalized burn ratio (NBR; Key and Benson, 2006) values and quantified post-disturbance responses using two spectrally derived indicators, the Relative differenced Normalized Burn Ratio (RdNBR; Miller et al., 2009) and the Recovery Indicator (RI; Kennedy et al., 2012; Fig. 2c). Because each stage provides the input for the next, uncertainty in disturbance detection and classification can propagate into recovery-metric estimates; therefore, the final resilience interpretation emphasises comparative spectral disturbance–recovery patterns and landscape-scale contrasts relevant to conservation assessment.

2.2.1. Data description

We acquired Landsat Tier 1 surface reflectance data for the CAT region for each dry season (June 1 to September 30) from 1984 to 2021. The data were harmonized across multiple Landsat sensors, including Landsat 5 Thematic Mapper (TM), Landsat 7 Enhanced Thematic Mapper Plus (ETM+), and Landsat 8 Operational Land Imager (OLI), using the equations provided by Roy et al. (2016). Clouds and cloud shadows were masked using FMASK-derived quality assurance bands (Zhu and Woodcock, 2012), and annual composites were generated using the medoid compositing method. The dry-season compositing window was selected primarily to reduce cloud contamination and also coincides with the main season of deforestation and fire (Da Veiga et al., 2025; Greenberg, 2026). Although this strategy may underestimate recovery signals associated with growing-season dynamics, it is a commonly used approach in tropical studies to ensure interannual data consistency.

We used the MapBiomas History of deforestation (MapBiomas, Collection 8), the MapBiomas History of Fire Scars (MapBiomas, Collection 3), and the Deforestation and Degradation in Tropical Moist Amazon forest (TMF) data from the European Commission's Joint Research Centre data products (Vancutsem et al., 2021) as reference data to aid in the preliminary selection of areas for the generation of the disturbance classification training and validation dataset. These products were used only to improve the efficiency of candidate sample selection. Final disturbance and vegetation labels were assigned through manual interpretation, so limitations of these reference products do not directly affect label accuracy. The key characteristics of these datasets are summarized in Table 2. In addition, we used vegetation survey plots from the Plant Ecology Laboratory of the Universidade do Estado do Mato Grosso as ground-based reference data to support the labelling of disturbance categories.

2.3. Identifying vegetation disturbance

Several regional and global disturbance-monitoring data products are freely available, including TMF, MapBiomas, Global Forest Change (Hansen et al., 2013), and near-real-time disturbance alert systems such as GLAD (Global Land Analysis and Discovery; Hansen et al., 2016) and RADD (Radar for Detecting Deforestation; Reiche et al., 2021). These datasets provide important insights into forest loss and recent disturbance events across the tropics, but are typically designed for specific monitoring objectives, such as humid forest systems, land-cover change detection based on classification transitions rather than continuous spectral disturbance signals, or rapid alerts over relatively short time spans. As a result, they may not fully capture long-term disturbance histories and recovery dynamics across ecotonal landscapes, where vegetation structure, fire regimes and degradation processes differ from those of closed-canopy forests.

To characterise disturbance and post disturbance recovery across the heterogeneous forest–savanna mosaics of the CAT, we therefore developed a dedicated disturbance dataset using multi-decadal Landsat time series. Specifically, we applied the LandTrendr time segmentation and fitting algorithm within GEE to detect vegetation disturbances within the CAT based on time series trajectories of the NBR. The LandTrendr algorithm operates on the principle that the temporal evolution of a pixel can be approximated by a series of linear segments. The algorithm's output is a fitted spectral trajectory represented by multiple interconnected segments for each pixel within the study area (Fig. 3; Kennedy et al., 2010). Building on this segment-based representation, LandTrendr provides temporally smoothed yet interpretable trajectories that reduce short-term noise while preserving key change features, which facilitates the extraction of disturbance and recovery segments for subsequent analysis. In addition, LandTrendr was implemented using annual composite imagery, which is well suited to cloud-prone tropical regions and provides temporally standardised, fixed-length time series inputs for downstream classification.

The selection of appropriate model parameters for the LandTrendr algorithm is crucial for accurate processing (Kennedy et al., 2010, 2018). For the algorithm-running parameters, we adopted LT-GEE settings (Kennedy et al., 2018) as a baseline and then adjusted

Table 2
Key characteristics of reference datasets.

Dataset	Description	Method	Spatial scope	Source
MapBiomas history of deforestation	Estimates forest and non-forest vegetation loss across biomes based on pixel-wise land cover change.	Track year-to-year changes in land cover and land use by comparing Annual land cover/use maps (Collection 8)	Brazil-wide	https://brasil.mapbiomas.org/en/metodo-desmatamento/
MapBiomas history of fire scars	Detects fire scars using burned/unburned samples and deep learning. But it does not distinguish between the types of vegetation where fires occur.	Deep Neural Network on Landsat imagery samples, with reference to MODIS burned areas product (MCD64A1) and burn scars from INPE	Brazil-wide	https://brasil.mapbiomas.org/en/metodo-mapbiomas-fogo/
TMF dataset	Tracks deforestation and degradation trajectories over 34 years using Landsat time series. But it does not include savanna regions like the Cerrado biome.	Spectral-temporal trajectory analysis from Landsat (1990–2024)	Global tropical humid forests	https://forobs.jrc.ec.europa.eu/TMF/data#factsheets

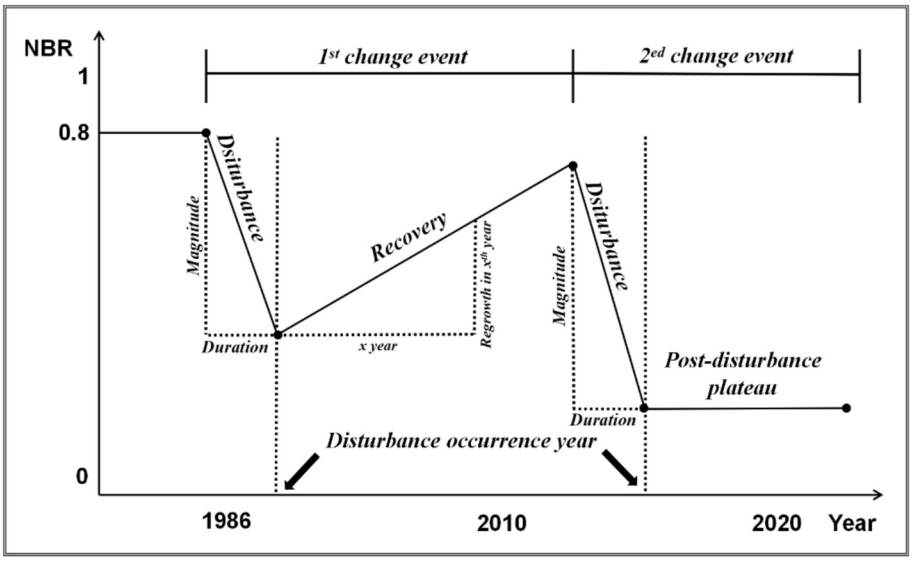

Fig. 3. Conceptual example of the disturbance and post disturbance NBR fitted trajectory. Concept example showing two change events at the same location, with quantitative indicators of disturbance and recovery.

maxSegments, recoveryThreshold, and spikeThreshold, because these parameters affect trajectory complexity, recovery constraints, and spike suppression, and therefore influence the detection of repeated disturbance events (Kennedy et al., 2010; Tu et al., 2024). To improve the representation of multiple disturbance events, we used a relatively flexible trajectory configuration (maxSegments = 9, recoveryThreshold = 0.75) to avoid over-constraining recovery segments in fast-recovering systems, where ecologically meaningful signals may otherwise be filtered out (Kennedy et al., 2010). Furthermore, considering the trade-off between noise suppression and oversmoothing abrupt disturbances, we set spikeThreshold = 0.75. The specific selection of all parameters was informed by LandTrendr guidance, technical reports, and prior calibration studies (Qiu et al., 2023; SERVIR-Amazonia, 2023; Tu et al., 2024; USDA Forest Service, 2023). A sensitivity analysis evaluating disturbance detection performance under alternative parameter configurations is provided in Appendix A and supports the robustness of the disturbance detection results used in subsequent analyses.

For the disturbance identification thresholds, we applied additional NBR-based constraints to reduce false positives and improve ecological interpretability. Specifically, we required pre-disturbance NBR > 0.2 to exclude non-vegetated or sparsely vegetated backgrounds, and disturbance magnitude >0.15 to retain meaningful disturbance signals while avoiding classification of minor fluctuations as disturbance. We also constrained disturbance duration <2 years because this study targets abrupt disturbances (mainly deforestation and fire) rather than gradual vegetation degradation. These parameter values and thresholds were checked through trajectory-based visual inspection of geographically distributed pixels in the GEE LandTrendr UI (eMapR Lab, 2018).

We define each change event as consisting of two components: (i) a disturbance segment, characterized by a negative trend in the NBR time series, and (ii) a post-disturbance segment, which follows one of two temporal trajectories (Fig. 3). The first trajectory is recovery, defined as a positive NBR trend after the disturbance until a subsequent disturbance is detected in the same pixel. The second is a post-disturbance plateau, defined as an approximately stable NBR value with no detectable recovery, typically associated with conversion to agriculture or pasture where natural vegetation regeneration is suppressed by continued human activity.

Where multiple disturbance events occurred in the same location but in different years, we repeated the analysis outlined above to obtain information for each disturbance event. We reported only disturbances occurring in 1986–2020, ensuring $\geq$2 years of pre- and post-disturbance observations for each breakpoint. This reduces endpoint-related uncertainty, as LandTrendr performance may degrade near the beginning and end of a time series (Guo et al., 2022; Oeser et al., 2017). As our study focused on disturbances to natural vegetation, as opposed to disturbances caused by clear-cutting of secondary forests or pasture fires, prior to analysis we masked all areas of non-forest and non-savanna vegetation that were present before 1985 using land use and land cover type data from Mapbiomas. In the subsequent disturbance classification process (see Section 2.2.3), we also excluded all disturbance events detected after a clear-cutting event was identified as the land cover post disturbance is likely to be different to that which was originally disturbed (e.g. clear-cutting of a forest for agricultural purposes is unlikely to result in the subsequent re-growth of a similar forest in the same location). Fire disturbances do not necessarily result in land use type conversions (Andela et al., 2017); therefore, secondary disturbances occurring after fire events were retained for analysis. After applying

these filtering steps, pixels experiencing more than three disturbance events accounted for only approximately 0.2% of all disturbed pixels (Appendix B, Table B1). Given their extremely limited spatial extent and the absence of clear spatial clustering, our analysis focuses on a maximum of three disturbance events per pixel.

We followed a probability-based design (Olofsson et al., 2014) to evaluate the accuracy of vegetation disturbance detection results. Reference samples were selected using simple random sampling across the CAT, and post-stratification by the disturbance detection map was applied at the estimation stage. We first determined the sample size per reference class (disturbed and undisturbed) according to the formula of Cochran (1977):

$$n = \frac{z^2 p(1-p)}{d^2} \quad (1)$$

with $z = 1.96$ (representing a 95% confidence interval), $d = 0.04$ (the desired half-width of the confidence interval), and $p = 0.94$ (expected overall accuracy from Reygadas et al., 2021), yielding 135 samples per class. This choice targets a ± 4% half-width at 95% confidence while keeping manual interpretation feasible, and equal allocation ensures sufficient support for each stratum and for class-specific accuracy estimates. Reference labels were assigned independently using TimeSync (Cohen et al., 2010) on Landsat time series, complemented by Google Earth high-resolution imagery. For pixels exhibiting multiple disturbance episodes during the study period, we validated the occurrence of the first disturbance. We finally report an area-weighted (probability) error matrix together with stratified, design-based estimates of overall, user's, and producer's accuracies, as well as area-adjusted estimates of the proportion of disturbed and undisturbed classes.

2.4. Classification of disturbance events

We aimed to classify four types of vegetation disturbance events based on the temporal trajectories of disturbance pixels identified by the LandTrendr algorithm (Table 3). In the CAT, most large-scale disturbance that can be reliably mapped with 30 m Landsat data is associated with clear-cut and recurrent fires (Miettinen et al., 2015; Morton et al., 2013; Pivello, 2011), whereas other agents such as selective logging or drought-related canopy stress tend to be more spatially localized and harder to detect consistently (Dalagnol et al., 2023; Matricardi et al., 2010). We therefore focus on clear-cutting and fire in forest and savanna ecosystems as the most extensive and policy-relevant disturbance types in the CAT.

To construct robust training and validation datasets for this classification task we first used the MapBiomas deforestation and fire products, as well as the TMF dataset (Section 2.2.1), to identify areas with a high likelihood of disturbance. This spatial filtering step reduced the search space and improved the efficiency of sample selection. Within these candidate areas, we randomly selected sample points that had also been independently detected as disturbances by the LandTrendr algorithm (Section 2.2.2), thereby ensuring consistency with our time series-based disturbance framework. For each selected sample point we used the TimeSync tool to manually verify and classify both the vegetation type and the specific disturbance category based on Landsat time series, Google Earth high-resolution imagery and vegetation survey plots. Label assignment was based on the combined interpretation of disturbance timing, spectral trajectory shape, and high-resolution visual context, and only samples with clear and consistent evidence across these sources were retained. To reduce mislabeling risk, we excluded ambiguous samples, including points located near vegetation patch edges. To mitigate potential sampling bias and ensure an even spatial distribution, we applied a minimum distance constraint of 300 m between selected points, which also helped reduce spatial autocorrelation among samples. Ultimately, we obtained a balanced dataset by selecting 2000 pixels for each of the four disturbance categories. These labelled samples were randomly split into training (80%) and validation (20%) datasets for model development and evaluation. The 20% subset was used solely for model tuning; its count-based confusion matrix and F1 score is provided in Appendix C (Table C1).

Table 3
Classification and description of vegetation disturbance events.

Event type	Description
Amazon forest clear-cutting	The complete removal of forest cover in the Amazon biome, typically through land clearing, leaving the land devoid of trees.
Cerrado clear-cutting	The full removal of natural vegetation in the Cerrado biome, including both woody and grassy vegetation, usually for agricultural or land development purposes.
Amazon forest fire	The damage or degradation of Amazon forests caused by uncontrolled or deliberate fires, which may not result in complete deforestation but can lead to significant ecological disturbances.
Cerrado fire	The disruption of the natural balance in the Cerrado biome due to fire, which can alter vegetation composition and ecosystem function, but may not entirely eliminate plant cover.

In addition to the training and validation datasets used for model development, we created an independent test set to evaluate the map following Olofsson et al. (2014). Specifically, we applied Cochran's formula (formula 1) with $z = 1.96$, $p = 0.90$, and $d = 0.05$, yielding 138 samples per map class. Unlike the LandTrendr accuracy assessment (which used post-stratification), this classification accuracy assessment used an a priori stratified design, with an equal number of samples drawn from each map class. We then implemented stratified simple random sampling within the four disturbance categories and, computed area-weighted (probability) error matrices and design-based OA, UA, and PA, as well as area-adjusted estimates of the proportion of each category. Reference labels for this test set were also assigned independently using TimeSync on Landsat time series, Google Earth high-resolution imagery and vegetation survey plots.

We used the 1D ResNet to classify the disturbance category based on the temporal trajectories of disturbance pixels identified using the LandTrendr algorithm. Unlike traditional machine learning approaches that rely on hand-crafted temporal features, 1D ResNet learns discriminative patterns directly from spectral trajectories. Its residual connections improve training stability and mitigate performance degradation with increasing network depth (He et al., 2015). Compared with recurrent models, 1D ResNet is also well suited to capturing local temporal patterns (Pelletier et al., 2019), such as abrupt spectral declines and rapid recovery, which are key signals for disturbance-type differentiation. This model class has been widely used in satellite image time series classification, particularly for crop and vegetation mapping (Li et al., 2023; Rußwurm and Körner, 2020; Simoes et al., 2021; Vanpoucke et al., 2024).

Specifically, we used a 1D ResNet architecture implemented in the Python TensorFlow library, following the ResNet-50 design described in Koonce (2021). The model was trained using a batch size of 64, where each sample corresponds to a 90 length time series vector representing a single pixel. We used a learning rate of $\eta = 0.001$ and optimized the model with the Adaptive Moment Estimation (Adam) algorithm for mini-batch gradient descent. The number of training epochs was set to 30 based on the convergence behaviour and stability of performance on the training and validation sets, in order to reduce the risk of overfitting. For each training pixel the temporal trajectories of three spectral bands and six spectral indices derived directly from the annual Landsat composites (Table 4) were used as inputs to the classifier, as previous studies have shown that including multiple spectral indices can reduce noise and improve classification accuracy (Shimizu et al., 2019). For pixels identified by the LandTrendr algorithm as having experienced a single disturbance within the study period, the time series trajectory began the year before the date that the disturbance was detected and continued for 10 years afterward. The 10-year time frame was selected based on the

Table 4
Spectral bands and vegetation indicators used for vegetation disturbance monitoring and classification, Blue, Green, Red are the visible blue, visible green and visible red bands, respectively.

Name	Abbreviation	Formula/band range	Features	Reference
Near-Infrared Reflectance	NIR	0.75–1.4 μm	Sensitive to chlorophyll content of living vegetation.	Avery and Berlin, 1992; Miller and Thode, 2007
Shortwave Infrared 1	SWIR1	1.55–1.75 μm	Sensitive to water content in soil and vegetation, lignin content of non-photosynthetic vegetation, and hydrous minerals.	
Shortwave Infrared 2	SWIR2	2.08–2.35 μm		
Normalized Burn Ratio	NBR	$NBR = \frac{NIR - SWIR2}{NIR + SWIR2}$	Not easily saturated and sensitive to viable chlorophyll, leaves, soil moisture content, char and ash. Responses to different types of disturbance (e.g., vegetation clear-cutting, fire, pests and diseases, etc.) are evident.	Bright et al., 2019; Key, 2006; Key and Benson, 2006; Schroeder et al., 2011
Normalized Difference Moisture Index	NDMI	$NDMI = \frac{NIR - SWIR1}{NIR + SWIR1}$	Highly correlated with canopy water content, it can track changes in plant biomass and water stress and therefore respond more effectively to less severe disturbance events.	DeVries et al., 2015; Gao, 1996; Ochtyra, 2020
Tasseled Cap Brightness	TCB	$\begin{bmatrix} TCB \\ TCG \\ TCW \end{bmatrix} = \begin{bmatrix} 0.2043 & 0.4158 & 0.5524 & 0.5741 & 0.3124 & 0.2303 \\ -0.1603 & -0.2819 & -0.4934 & 0.7940 & -0.0002 & -0.1446 \\ 0.0315 & 0.2021 & 0.3102 & 0.1594 & -0.6806 & -0.6109 \end{bmatrix} \begin{bmatrix} Blue \\ Green \\ Red \\ NIR \\ SWIR1 \\ SWIR2 \end{bmatrix}$	TCB provides an indication of the overall pixel reflectance, TCG provides an indication of vegetation photosynthetic conditions, and TCW is highly sensitive to changes in Amazon forest structure.	Banskota et al., 2014; Crist and Cicone, 1984; Healey et al., 2006
Tasseled Cap Greenness	TCG			
Tasseled Cap Wetness	TCW			
Tasseled Cap Angle	TCA	$TCA = \arctan\left(\frac{TCG}{TCB}\right)$	TCA reveals the ratio of vegetation to non-vegetation, with TCA in harvested areas being significantly lower than in any other Amazon forest cover stage.	Gómez et al., 2011; Schroeder et al., 2011

results of Chen et al. (2021), which demonstrated that a 10-year time frame has a lower error rate than other time series lengths in monitoring and classifying deforestation and fire events by convolution neural network. In cases where multiple disturbances were detected, separate time series trajectories were extracted for each event. To handle cases where the time series trajectory was shorter than 10 years, such as disturbances occurring after 2012 or in pixels that experienced subsequent disturbances within a 10-year window, the final year of the trajectory was replicated to ensure a uniform time series length across all samples. The ResNet model primarily captures local features via convolutional layers and is less sensitive to the sequence order (Wei-Jian et al., 2021), thus we concatenated the nine time series trajectories for each pixel (corresponding to three bands and six indices) into a single sequence of length of 90 to simplify its structure for improved computational efficiency. All time-series samples were normalized to the range −1 to 1 in order to accelerate model convergence and stabilize training (Salimans and Kingma, 2016).

2.5. Disturbance and recovery trajectory analysis

We generated quantitative trajectory indicators from the model-fitted NBR time series to understand how vegetation within the CAT responded to different types of disturbance events. For each disturbance event that we identified (Sections 2.3 and 2.4), we calculated two key indicator trajectories. The first index quantified the level of vegetation damage caused by the disturbance, as it uses pre and post disturbance values of NBR to calculate the RdNBR, which determines the relative change in vegetation post disturbance (eq. 2).

$$RdNBR = \frac{\Delta NBR}{\sqrt{ABS(NBR_{predis})}} \quad (2)$$

Where ΔNBR is the NBR change in disturbance, NBR_{predis} is the absolute value (non-negative) of NBR before disturbance.

We compared the RdNBR among the four disturbance categories using one-way analyses. After assessing analysis of variance (ANOVA) assumptions (normality of model residuals and homogeneity of variances), we applied Welch's one-way ANOVA with Games–Howell post-hoc comparisons to provide inference robust to heteroscedasticity.

We also calculated the RI, which quantifies the degree of vegetation recovery following a disturbance event The RI is the ratio of post-disturbance regrowth to the level of vegetation lost during the preceding disturbance event (Eq. 3). Since clear-cutting typically signifies a land-use conversion, which precludes vegetation recovery, the RI metric was only calculated for fire events. We standardised post-disturbance recovery assessment to a 10-year window to provide a consistent basis for comparing recovery across disturbance types, vegetation contexts, and event years in the CAT. Preliminary analysis indicated that year-to-year variation in NBR became limited beyond 10 years. This choice is also consistent with previous studies showing that recovery is often most dynamic in the first post-disturbance decade in many forest systems (Pickell et al., 2016; Senf et al., 2019; White et al., 2018), while Cerrado vegetation can also show rapid early recovery after fire (Konduri et al., 2023; Machida et al., 2021). If the recovery period was shorter than 10 years, the RI was calculated up to the final year of the available recovery trajectory.

$$RI = \frac{NBR_{y+x} - NBR_y}{\Delta NBR} \quad (3)$$

where NBR_y is the NBR value in the disturbance year y, and NBR_{y+x} is the NBR value in the xth year after the disturbance. RI is interpreted as an NBR-based spectral recovery indicator, representing the proportion of post-disturbance recovery in canopy greenness and related canopy attributes relative to the disturbance-induced loss. From an ecological perspective, RI is not a direct measure of full ecosystem recovery; however, NBR change have been widely linked to field-observed fire effects and vegetation structural change, such as Composite Burn Index, canopy cover change, and basal area change (Bright et al., 2019; Epting

et al., 2005; Miller et al., 2009; Morresi et al., 2022), and RI have also been widely used to characterise post-fire vegetation recovery dynamics (Kennedy et al., 2012; Pérez-Cabello et al., 2021; White et al., 2017). Therefore, RI is used here as a proxy for post-fire recovery dynamics and resilience-related responses.

3. Results

3.1. Reliability and regional variation of disturbance detection

Despite the diverse vegetation types present in the CAT zone, the LandTrendr algorithm achieved an overall disturbance detection accuracy of 0.79 (95% CI: 0.74–0.84; Table 5). Whilst some disturbed pixels were not identified (~33%) by the LandTrendr algorithm, 86% of the pixels that were identified as disturbed were correct compared with the reference data. These results suggest that while our estimates of disturbance within the CAT region may be underestimated, we have a high degree of confidence that the pixels identified as disturbed accurately represent true disturbances.

Over the 35-year period, an estimated 493,050 km^2 of the CAT experienced at least one disturbance. Given that approximately 33% of disturbed pixels were not identified by the LandTrendr (Table 5), this estimate should be interpreted as a conservative statistical lower bound. Fig. 4 presents the spatial patterns of disturbance events and the years in which each disturbance was detected. The most recent disturbance events were found to the far north of the CAT dividing line toward the natural vegetation of the Amazon biome, and also tend to be spatially clustered (Fig. 4a). In contrast, disturbances in the region south of the CAT boundary in the Cerrado biome were more temporally heterogeneous and their spatial distribution was more dispersed (Fig. 4b). These spatial patterns delineate clear disturbance hotspots, with clusters of disturbance particularly pronounced near major farming and ranching landscapes in the Amazon forest, whereas Cerrado disturbances are more diffuse and scattered.

3.2. Identifying different types of vegetation disturbance

Our findings indicate that disturbance categories can be mapped with good overall accuracy using temporal disturbance trajectories in conjunction with the ResNet classification architecture, achieving an overall classification accuracy of 0.83 (95% CI: 0.80–0.87; Table 6). Inspection of the largest off-diagonal elements suggests minor confusion between some class pairs, primarily between the two fire classes, with additional errors where Cerrado clear-cutting is occasionally misclassified as Cerrado fire and Amazon forest clear-cutting as Cerrado clear-cutting. Fig. 5 provides examples of the temporal trajectories that are characteristic of different mapped disturbance categories. Amazon forest clear-cutting and fires resulted in more pronounced changes in spectral and vegetation indicators compared to disturbance observed in the Cerrado vegetation. Clear-cutting in both the Amazon forest and Cerrado vegetation resulted in more abrupt and longer-lasting change in spectral and vegetation indicators compared to fire disturbances. Among all indicators, NBR and NDMI exhibited the most pronounced changes in magnitude between pre- and post-disturbance conditions, regardless of the disturbance category.

Our disturbance classification results show that Amazon forest clear-cutting was the main type of disturbance in the CAT zone between 1986 and 2020 and accounted for 35% of the total disturbed area. Forest clear-cutting was widespread across the CAT and frequently found north of the traditional ecological boundary (Fig. 6 and 7a). In contrast to wide-spread forest clear-cutting, forest disturbances caused by fire tended to be more spatially clustered, smaller in size, and often located adjacent to forested areas that had been clear-cut (Fig. 6a). Forest fires were also often observed along river corridors (Fig. 6b). Together, these clusters define compound disturbance hotspots, where clear-cutting and fire co-occur and reinforce degradation patterns.

Unlike Amazon forest disturbances, our results showed that disturbances that occurred in Cerrado vegetation were primarily in the southern part of the CAT. Cerrado disturbances were often smaller than those occurring in Amazon forest vegetation and were distributed across the landscape in a scattered and irregular manner (Fig. 6a). However, similar to Amazon forest vegetation, a clear spatial association was observed between disturbed Cerrado vegetation affected by clear-cutting and fire, indicating spatial co-occurrence of these disturbances (Fig. 7b and d). In the Cerrado, these high-frequency pixels correspond to more diffuse disturbance hotspots embedded in a fragmented mosaic, which may be harder to detect and manage than the more contiguous hotspots observed in Amazon forest.

Fig. 8 illustrates the temporal dynamics of the Amazon forest and Cerrado disturbances between 1986 and 2020. Our results show a positive trend in the total disturbed area prior to 1998 followed by another increase in the area affected by clear-cutting in the Amazon forest vegetation between 2002 and 2004 (Fig. 8a). Our analysis also indicates that in the Amazon forest vegetation, an increase in the area disturbed by fire following increases in the area disturbed by clear-cutting, suggesting a potential lagged relationship (Fig. 8a); whereas in the Cerrado vegetation, the area affected by both types of disturbances show a synchronous temporal pattern (Fig. 8b).

3.3. Influence of the type of disturbance on vegetation disturbance-recovery trajectories

We calculated the RdNBR to quantify and compare the level of vegetation damage due to different types of disturbance events. Our results indicate that the vegetation damage of the disturbance endured differs according to the type of disturbance event (Table 7; Welch's $F = 336.58$, $df = 3, 30{,}803$, $p < 0.001$). As expected, we found that on average, fire disturbances were associated with lower vegetation damage, as indicated by lower RdNBR values, compared to clear-cutting, in both Cerrado vegetation and Amazon forest vegetation within the CAT (Fig. 9). Our results also suggest that many of the fire disturbances identified within the Amazon forest vegetation were of low damage, compared to those observed in the Cerrado vegetation, whereas clear-cutting had a very similar impact on both types of vegetation communities (Fig. 9).

We also compared the recovery of vegetation cover in Amazon forest and Cerrado vegetation following fire disturbance, as indicated by changes in the annual RI. Our findings revealed that vegetation began to regrow quickly within both the Amazon forest and Cerrado vegetation, recovering to approx 80% of pre-fire levels in the Amazon forest vegetation by the end of the time series, but only 60% of the pre-fire levels in the Cerrado vegetation (Fig. 10). Notably, neither vegetation type fully returned to pre-disturbance conditions within a ten-year period, as indicated by an annual RI value < 1.

Table 5
Area-weighted (probability) error matrix and population accuracy for disturbance identification in the CAT region. 95% confidence intervals in parentheses; Because values are reported to two decimal places, the sum of rounded cell entries may not exactly match row/column totals calculated from the unrounded estimates.

	Reference disturbed	Reference undisturbed	Row total
Map disturbed	0.32	0.05	0.37
Map undisturbed	0.16	0.47	0.63
Column total	0.47	0.53	
Overall accuracy		0.79 (0.74 to 0.84)	
User's accuracy (disturbed)		0.86	
User's accuracy (undisturbed)		0.75	
Producer's accuracy (disturbed)		0.67	
Producer's accuracy (undisturbed)		0.90	
True disturbed proportion		0.47 (0.42 to 0.52)	

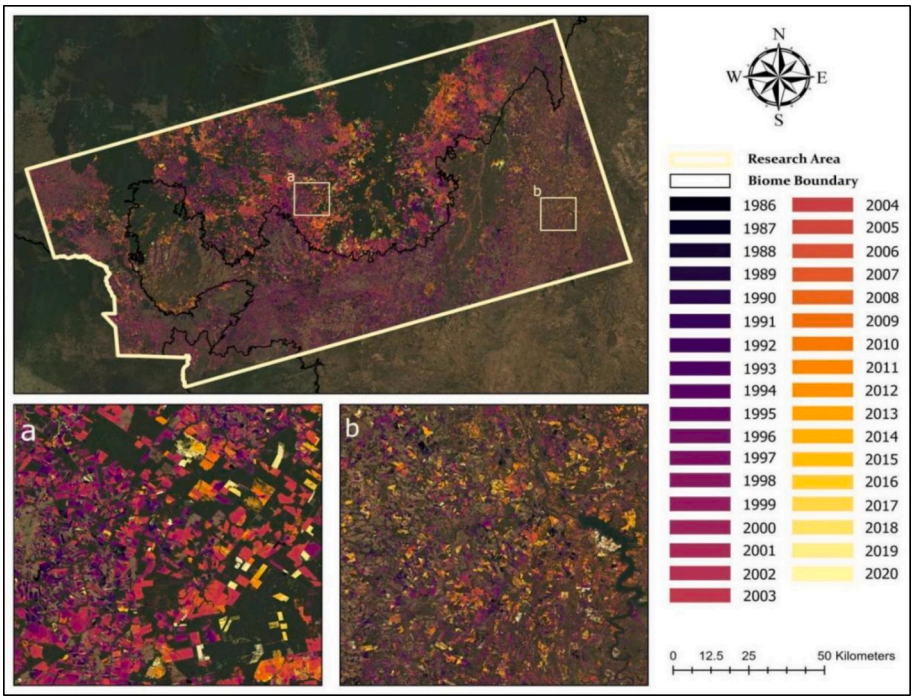

Fig. 4. Spatial distribution of the timing of first vegetation disturbance occurrence in the CAT between 1986 and 2020. Insets illustrate regional spatial details. Darker concentrations of disturbed pixels indicate disturbance hotspots, particularly near major farming and ranching landscapes in the Amazon forest (a), whereas Cerrado disturbances (b) are more diffuse. The Cerrado panel was chosen because of it highlights the heterogeneous pattern of disturbance events and the diverse landscape characteristics of this biome. The background image is a composite of cloud-free Landsat 8 OLI scenes acquired between Jan 1 and Dec 30, 2021.

Table 6
Area-weighted (probability) error matrix and population accuracy for disturbance type classification in the CAT region. 95% confidence intervals in parentheses; Because values are reported to two decimal places, the sum of rounded cell entries may not exactly match row/column totals calculated from the unrounded estimates.

		Reference				Row total
		Amazon forest clear-cutting	Cerrado clear-cutting	Amazon forest fire	Cerrado fire	
Predicted	Amazon forest clear-cutting	0.30	0.01	0.03	0.01	0.35
	Cerrado clear-cutting	0.03	0.16	0.00	0.00	0.19
	Amazon forest fire	0.01	0.01	0.18	0.03	0.21
	Cerrado Fire	0.01	0.03	0.02	0.19	0.24
Column total		0.35	0.20	0.22	0.23	
Overall accuracy		0.83 (0.80 to 0.87)				
User's accuracy		0.86	0.85	0.82	0.80	
Producer's accuracy		0.88	0.80	0.80	0.83	
Estimated true class proportion		0.35 (0.32 to 0.37)	0.20 (0.18 to 0.22)	0.22 (0.19 to 0.24)	0.23 (0.21 to 0.25)	

4. Discussion

4.1. Disturbance detection in a complex tropical ecotone

The CAT represents an ecotonal region of exceptional ecological significance, where the Amazon forest and Cerrado vegetation converge to create a heterogeneous landscape that supports high biodiversity (Maracahipes-Santos et al., 2015; Marques et al., 2020). Using the novel combination of time series analysis of EO data together with a deep learning model, our study provides a unique insight into the extent and intricate spatial patterns of vegetation disturbances within the ecologically sensitive CAT region over the last 35 years.

With the increasing length of EO data records, time series-based vegetation monitoring techniques offer expanded opportunities for studying disturbances. We show that the LandTrendr algorithm in combination with the ResNet model can be used to detect and classify vegetation disturbances in complex spatially heterogeneous ecosystems with a high level of overall accuracy (79% and 83%; Tables 5 and 6). The reported overall accuracy are comparable to those from deep learning applications in more homogeneous Amazonian forests and savanna–forest mosaics (Bendini et al., 2022; Dalagnol et al., 2023; Maretto et al., 2020; Mota et al., 2024), further supporting the robustness of our approach in a dynamic ecotone such as the CAT. By pre-structuring disturbance trajectories with LandTrendr, our two-step framework also reduces training data requirements and enhances scalability for regional, multi-year disturbance monitoring.

However, the relatively lower producer's accuracy for the Disturbed (67%) indicates that our disturbance detection is conservative. This likely reflects two main factors. First, LandTrendr detection consistency is sensitive to parameter and threshold choices across vegetation types. This creates a trade-off between suppressing spectral noise in closed-canopy forest and retaining sensitivity to lower-intensity disturbances in structurally open Cerrado vegetation, which may lead to omission of subtle Cerrado disturbances. Second, because we used annual composites, temporally proximate or overlapping disturbances may be represented as a single dominant disturbance signal. In contrast, the corresponding user's accuracy (86%) indicates that we have high confidence in the disturbances identified by the framework. Therefore, omission error mainly introduces uncertainty in absolute disturbance extent or reduces sensitivity to disturbance frequency counts, rather than causing widespread inclusion of false disturbance signals in

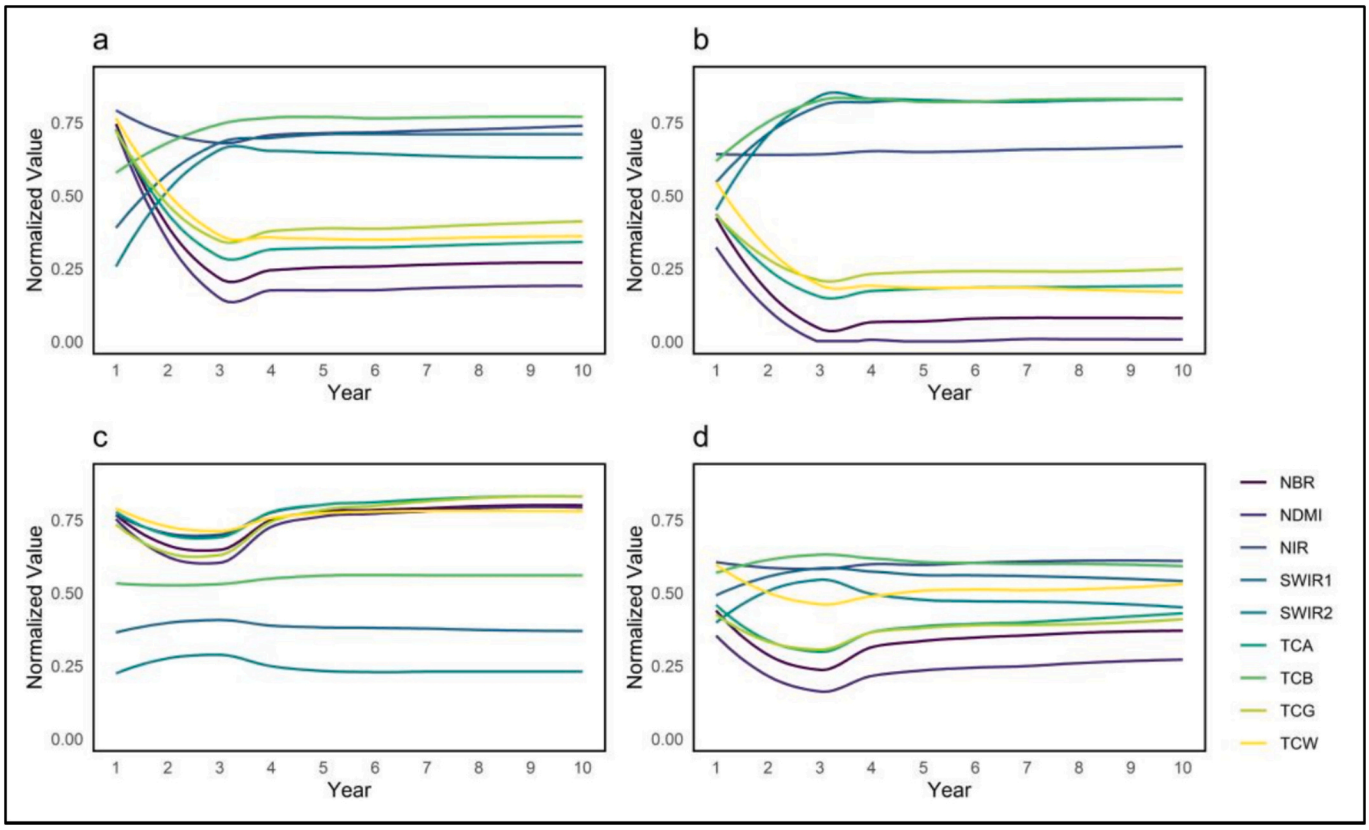

Fig. 5. Mean values of the time series of spectra and vegetation indicators for different vegetation disturbance categories in the disturbance classification model. (a) Amazon forest clear-cutting; (b) Cerrado clear-cutting; (c) Amazon forest fire; (d) Cerrado fire. Abbreviations are defined in Table 4.

downstream analyses.

Additionally, the classification results show minor confusion between specific class pairs (Table 6). Confusion across vegetation-related classes likely reflects the continuous forest–savanna gradient in the CAT, where high-canopy Cerrado physiognomies can be spectrally and structurally similar to forest formations, reducing separability in optical time series features (Alencar et al., 2020; da Cruz Silva et al., 2025; Li et al., 2025). Moreover, rapid post-fire regeneration of grasses and resprouting vegetation, can shorten or blur the spectral contrast among fire-related trajectories, increasing overlap between fire categories (Pilon et al., 2021; Vourlitis et al., 2026). However, the magnitude of these confusions is small (maximum off-diagonal proportion = 0.03), so their influence on downstream analyses is limited.

4.2. *Spatio-temporal patterns and socio-economic drivers of disturbance*

Using Landsat time series and the LandTrendr algorithm combined with a ResNet model, our results suggest that Amazon forest clear-cutting has been the cause of the most widespread disturbances within the CAT over the last 35 years, accounting for approximately 35% of the total disturbed area (Fig. 6). The Amazon forest clear-cutting gradually erodes the edges of intact vegetation (Fig. 4a). Driven largely by agricultural expansion, Amazon forest vegetation continued to be the primary target for conversion into croplands and pastures (Fig. 6). Similar patterns of persistent and large-scale clear-cutting have previously been observed along the so-called “Arc of Deforestation” and are often associated with the progressive incursion of agricultural zones into forested landscapes (Arvor et al., 2017; Matricardi et al., 2020; Ribeiro et al., 2025; Verburg et al., 2014). In the CAT, these dynamics generate pronounced disturbance hotspots along major farming and ranching landscapes, where repeated clear-cutting increasingly isolates remaining forest patches. Our results suggest that in the CAT, Amazon forest clear-cutting reached a peak around the year 1998 (Fig. 8a), and the underlying temporal dynamics are consistent with economic shifts, policy changes, and market conditions as plausible drivers of the observed spatiotemporal pattern. For example, the broader liberalization of Brazil's economy in the early 1990s and the introduction of the Real Plan in 1994, which stabilized inflation and attracted agribusiness investment, are often cited as factors that contributed to agricultural expansion across the Amazon and Cerrado biomes (Myers, 2023). Global commodity demand and rising crop prices during the late 1990s may have further accelerated land clearing during this period (Harding et al., 2021; Nepstad et al., 2006; Ouma, 2020). Following this peak, a decline in clear-cutting is observed after 2000 (Fig. 8a), which related to the Plano Real having sharply cut the rate of inflation. By the end of 1997, land prices reportedly dropped by around 50%, reducing the appeal of land speculation (Fearnside, 2005). Our results indicate that a second wave of Amazon forest clear-cutting emerged around 2004 (Fig. 8a). This timing coincides with evidence of a global surge in commodity demand and agricultural prices, which likely supported increased agricultural production in the CAT (Bacha and Vinicios de Carvalho, 2014; Harding et al., 2021; Nepstad et al., 2006; Ouma, 2020). Another possible contributing factor is the weakening of environmental oversight and enforcement capacity in the CAT region, which occurred around 2002 due to a significant reduction in IBAMA's field personnel and limited resources, leaving large areas without effective monitoring or control (Barreto, 2006). Notably, to this day, while protected areas currently cover approximately 28% of the Amazon biome, only 2% of this protection falls within the boundaries of our study area (according to conservation data from Mapbiomas), highlighting the CAT's institutional vulnerability (Carneiro et al., 2024; Pokorny et al., 2013, 2021; Pokorny and Pacheco, 2014; Ros-Tonen et al., 2008).

In contrast to the concentrated disturbance patterns observed in Amazon forest vegetation, our results show that disturbances to Cerrado

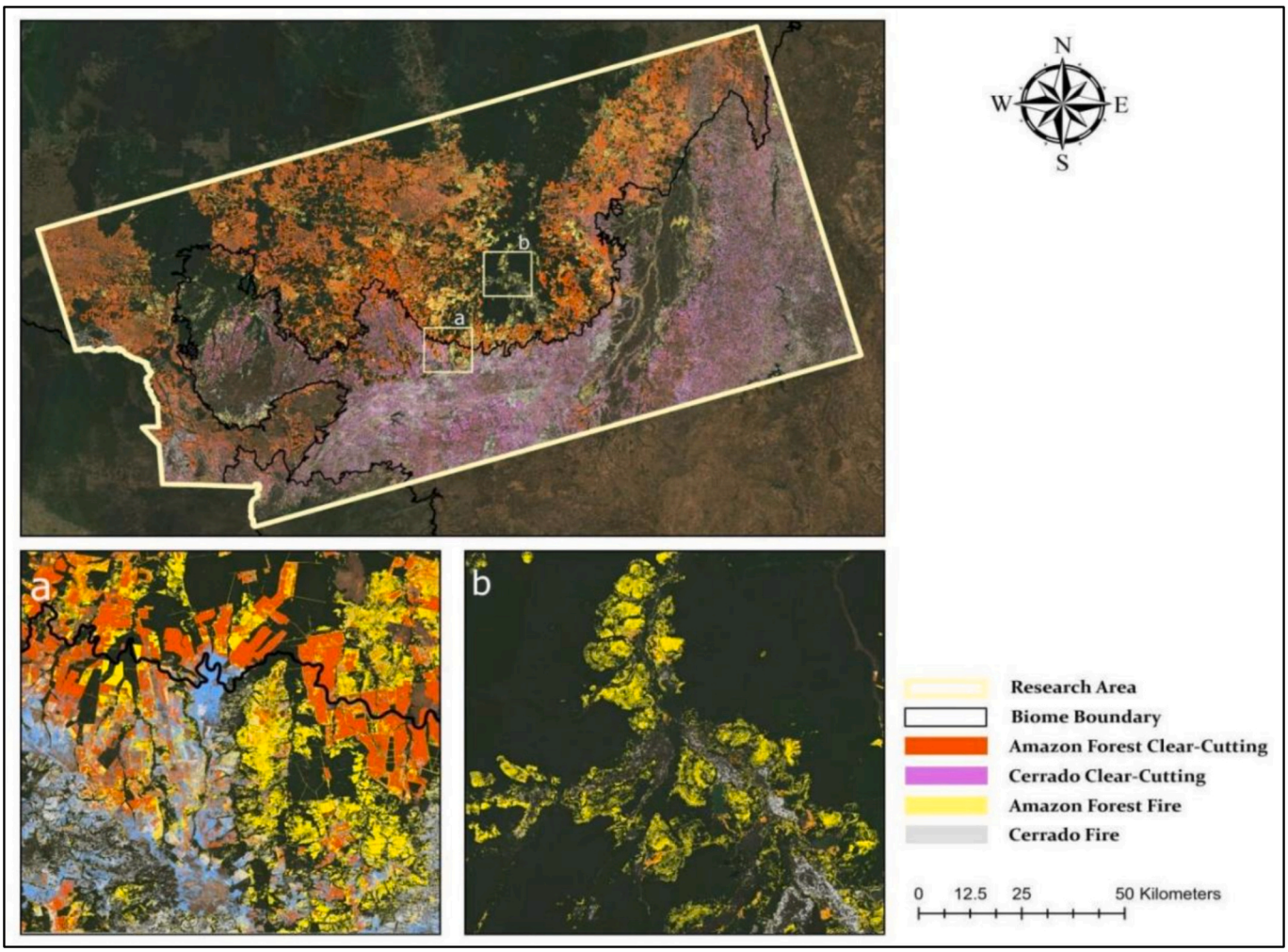

Fig. 6. Spatial distribution of first vegetation disturbance categories detected in CAT between 1986 and 2020 and examples of regional spatial details showing (a) fires occurring around clear-cutting areas and (b) fires occurring along rivers.

vegetation were spatially dispersed (Fig. 4b), which is consistent with the decentralized pattern of land conversion typically observed in the wider Cerrado biome (Rosan et al., 2022; Sawyer, 2008). Unlike Amazon forest vegetation, where large contiguous tracts are often targeted for conversion, land-use change in the Cerrado tends to occur in smaller, scattered patches. This reflects both the mosaic nature of Cerrado landscapes (Martello et al., 2023) and the decentralized expansion of agricultural frontiers (Sano, 2019). This diffuse pattern of land conversion creates scattered disturbance hotspots embedded within a highly fragmented matrix, making their detection and management particularly challenging. This pattern contributes to a subtler but persistent erosion of ecological integrity over time (Dionizio and Costa, 2019; Gomes et al., 2019; Lucas et al., 2023). A key factor shaping this process is the Cerrado biome's limited legal protection relative to the Amazon biome. While nearly 80% of the Amazon biome is covered by legal environmental frameworks, only 35% of the Cerrado biome within the "Legal Amazon" and 20% outside it fall under similar protection (Carneiro et al., 2024; Colman et al., 2024; De Marco Jr et al., 2023; Luiz and Steinke, 2022). The discrepancies in governance have resulted in uneven enforcement and monitoring efforts, allowing for continued expansion of agricultural activities in more vulnerable Cerrado biome. Our results show that by 1998 large-scale Cerrado clear-cutting had substantially reduced vegetation cover (Fig. 8; Marques et al., 2024; Vieira et al., 2022), leading to a subsequent decline in clearing activities in subsequent years.

Our results reveal a strong temporal and spatial association between clear-cutting and fire in both Amazon forest and Cerrado vegetation within the CAT (Figs. 7 and 8). This pattern is consistent with the intentional use of fire to expand grazing land and prepare soils for agriculture (Andreoni and Londoño, 2019; Arroyo-Kalin, 2012; Gomes et al., 2019; de Medeiros and Fiedler, 2011; Pivello et al., 2021). Fire disturbances were frequently located near pastures (Fig. 4c), and Amazon forest fires were often observed along riverbanks, some of which overlap with indigenous territories where traditional slash-and-burn practices persist (de Alencar et al., 2023; Golin, 2024; Schmidt et al., 2021). These coupled clear-cut-fire dynamics generate compound disturbance hotspots, where repeated burning and land conversion interact to accelerate degradation. Amazon forest fire activity typically peaked several years after clear-cutting, whereas Cerrado fire and clear-cutting tended to occur simultaneously (Fig. 8). This divergence reflects different land-management practices: in the Amazon, fire is commonly used as a post-clearing tool to manage regrowth and prepare land for pasture, while in the Cerrado it is more frequently employed directly for clearing and soil conditioning (Arroyo-Kalin, 2012; Gomes et al., 2019). Furthermore, fire activity is also sensitive to climatic variability, particularly drought conditions that increase fuel dryness and facilitate fire spread. For example, the 1998 peak is consistent with the strong 1997–1998 El Niño–related drought (Alencar et al., 2006). Likewise, the extreme Amazon droughts of 2005, 2010, and 2015 have been widely documented (Aragão et al., 2018; Marengo et al., 2008; Silva Junior et al., 2019). In CAT, the frequency of fire events increased to varying degrees during these drought years (Fig. 8).

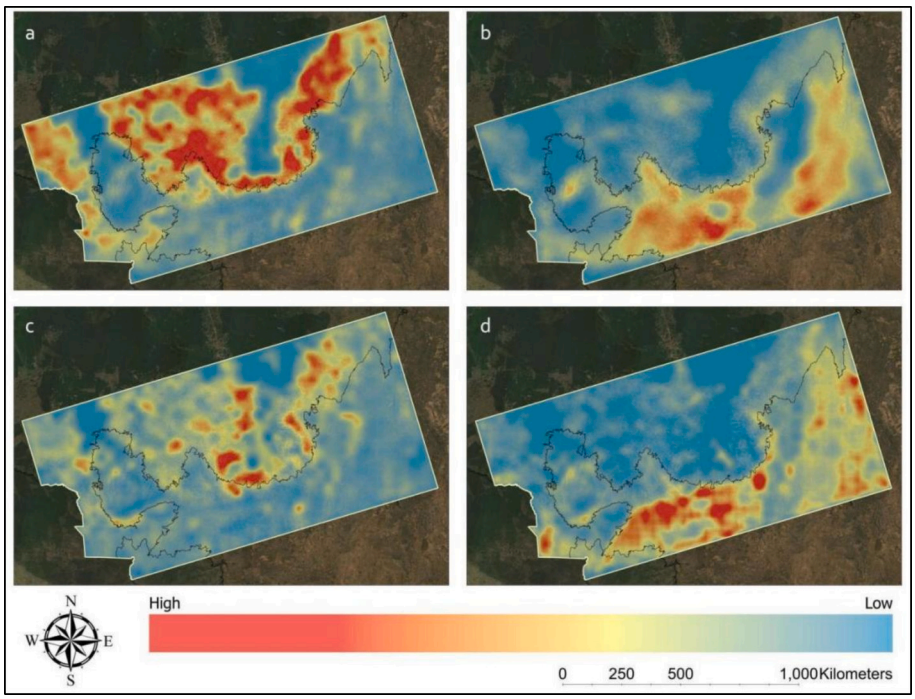

Fig. 7. Distribution of high frequency areas by disturbance category. (a) Amazon forest clear-cutting, (b) Cerrado clear-cutting, (c) Amazon forest fire, (d) Cerrado fire in the CAT. The maps were generated by interpolating the cumulative disturbance area within each 1000 × 1000-pixel grid cell (900 km^2). If multiple disturbances occurred at the same pixel during the study period, each event was included in the total area calculation.

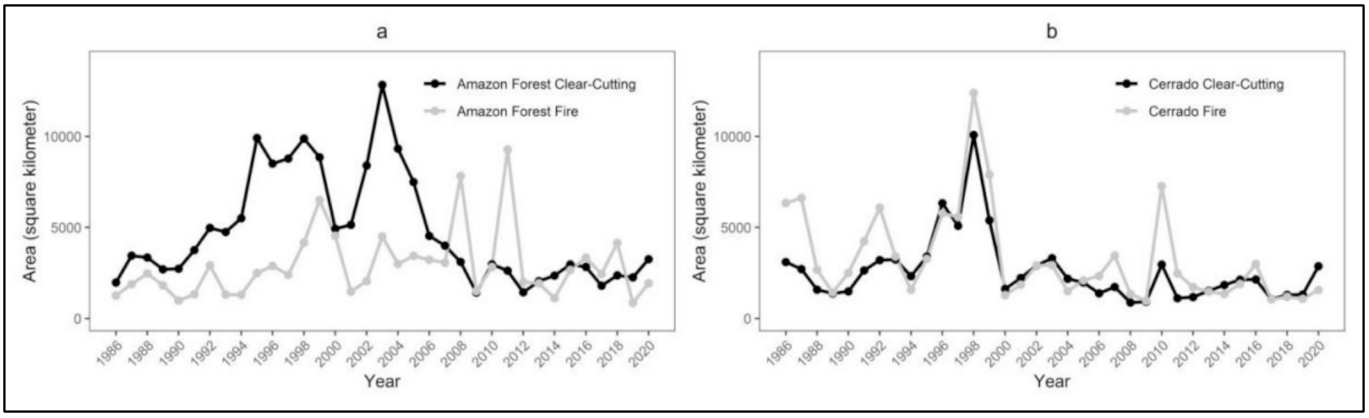

Fig. 8. Temporal dynamics of vegetation disturbance in the (a) Amazon forest vegetation and (b) Cerrado vegetation.

Table 7
Pairwise comparisons of RdNBR among disturbance types using Games–Howell test (Welch-adjusted).

Comparison		Mean difference	95% CI	Adjusted *p*
Amazon forest clear-cutting	Amazon forest fire	−0.152	[−0.165, −0.138]	<0.001
Amazon forest clear-cutting	Cerrado clear-cutting	−0.029	[−0.043, −0.015]	<0.001
Amazon forest clear-cutting	Cerrado fire	−0.047	[−0.061, −0.032]	<0.001
Amazon forest fire	Cerrado clear-cutting	0.122	[0.109, 0.136]	<0.001
Amazon forest fire	Cerrado fire	0.105	[0.092, 0.119]	<0.001
Cerrado clear-cutting	Cerrado fire	−0.017	[−0.032, −0.003]	0.011

4.3. Ecosystem responses, fire-driven degradation and resilience

Understanding how different vegetation types respond to disturbance is critical for evaluating ecosystem resilience and informing effective conservation and land management strategies. In this study, we employed trajectory-based indicators to quantify both the severity of vegetation damage and the rate of post-disturbance recovery across the Amazon forest and Cerrado within the CAT region, focusing specifically on disturbances caused by clear-cutting and fire. Our results reveal that fire events in the CAT tend to cause greater and more prolonged damage to Cerrado vegetation compared to adjacent forested areas (Fig. 9). To our knowledge, this is the first regional-scale, Earth observation-based study to compare fire impacts across these two contrasting vegetation types within the CAT. Although Cerrado ecosystems are often described as fire-adapted, previous studies indicate that their structural characteristics, such as open canopies and a grass-dominated understory, make them highly flammable (Durigan and Ratter, 2016; Miranda et al., 2009; Rodrigues et al., 2021). During the dry season, rapid desiccation and the

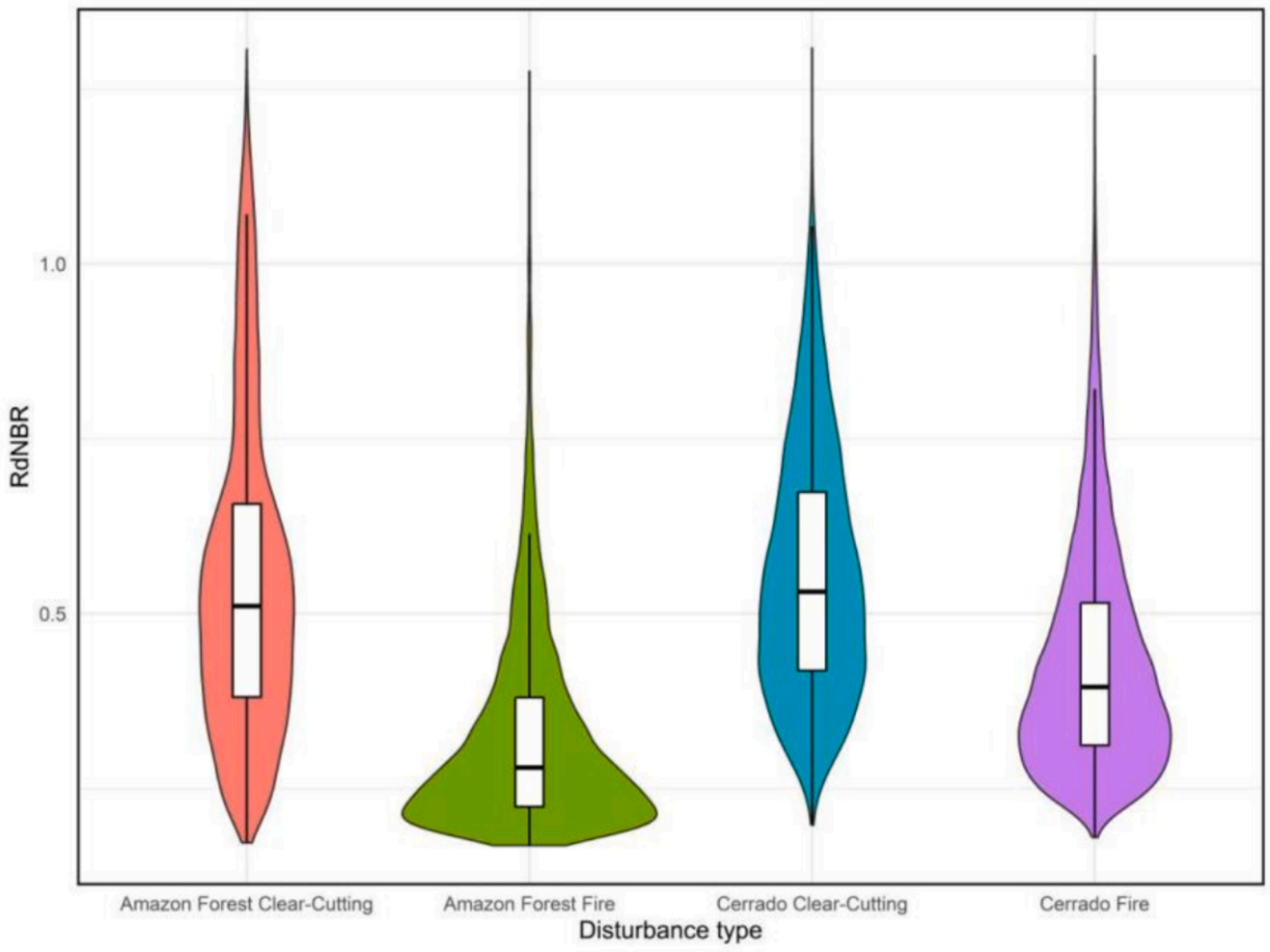

Fig. 9. A violin plot of the distribution of RdNBR values for the different disturbance categories in the CAT, based on 50,000 randomly sampled pixels.

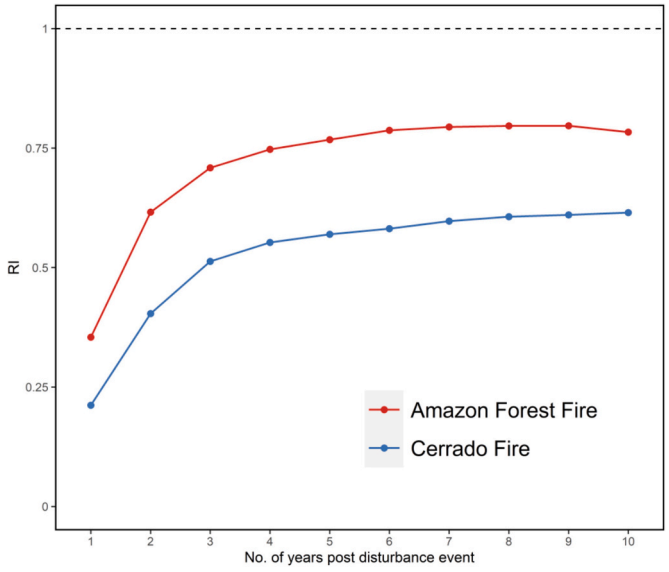

Fig. 10. Annual RI of different disturbance categories in the CAT. An RI value of 1 indicated that vegetation cover has returned to pre-disturbance levels. The plots have been generated from 50,000 randomly sampled pixels.

build-up of fine fuels significantly increase fire intensity, frequently resulting in widespread topkill of woody vegetation (Hoffmann et al., 2012).

This vulnerability is further amplified by human-induced ignitions, which have become increasingly frequent and severe in recent years (Alvarado et al., 2017; da Silva Arruda et al., 2024; Melo et al., 2021). Our findings provide empirical, landscape-scale evidence that supports these concerns and highlights the susceptibility of Cerrado vegetation to fire-driven degradation, even in regions where fire has historically been part of the disturbance regime. In contrast, the Amazon forest's closed canopy appears to buffer fire effects by preserving soil moisture and limiting the accumulation and exposure of fine fuels (Connell and Slatyer, 1977; Dormann et al., 2020). However, fire-induced losses beneath dense forest canopies may be underestimated by satellite sensors due to limited spectral penetration, suggesting that some impacts on forest structure and regeneration dynamics may remain undetected.

Both Amazon forest and Cerrado vegetation began to show spectral signs of post-fire recovery within approximately three years, but our results indicate that neither vegetation type returned to pre-fire levels even a decade after disturbance (Fig. 10), consistent with other regional studies (Silva et al., 2018; Souza-Alonso et al., 2022). This suggests that, although the first decade captures an important phase of post-disturbance recovery, the full recovery process may extend beyond 10 years, particularly under repeated fire and changing disturbance regimes (Drüke et al., 2023; Flores and Holmgren, 2021; Machida et al., 2021). For Amazon forest, incomplete recovery likely reflects the combined effects of increasing drought frequency and intensity and recurrent anthropogenic fires, which limit the time available for regeneration

between events (Alencar et al., 2011; De Faria et al., 2021a, 2021b). However, the fire-adapted Cerrado vegetation did not recover more rapidly or more completely than the Amazon forest. This finding challenges the conventional understanding that the Cerrado vegetation generally recovers more rapidly after fire (Hoffmann, 2005; Moreira, 2000) and suggests that recent changes in disturbance regimes, particularly repeated human-driven fires, may be pushing Cerrado ecosystems beyond their historical fire-adapted equilibrium (Alvarado et al., 2017; Hoffmann et al., 2012). The cumulative impacts of such fires reduce structural integrity, limit regeneration potential, and ultimately undermine long-term ecological resilience (Attri et al., 2020; Pinty et al., 2000; Souza-Alonso et al., 2022). In addition, recovery rates in the Cerrado are strongly influenced by fire frequency, severity, and species, which can lead to longer and more variable recovery trajectories than expected (Konduri et al., 2023; Machida et al., 2021; Reis et al., 2015).

The spatial clustering of disturbance hotspots (Fig. 7) and the recovery outcomes following fire (Fig. 10) also align with fire–vegetation feedbacks documented for tropical forest–savanna transition systems (Hirota et al., 2011; Staver et al., 2011). Recurrent burning driven canopy opening can favour grass expansion and greater fuel connectivity, increasing landscape flammability and reinforcing subsequent fire occurrence (Silvério et al., 2013). When compounded by episodic drought and warming conditions, these feedbacks may be amplified, eroding recovery capacity and increasing the risk of threshold-like shifts toward a more open, fire-prone state within the forest–savanna transition zone (Brando et al., 2014).

It is also important to note that recovery detected by satellite imagery mainly reflects increases in canopy greenness, rather than full ecological recovery of pre-fire ecosystems. In this context, increasing RI values indicate progressive post-fire spectral recovery relative to the initial disturbance-induced loss, but this should be interpreted as recovery of spectral signals rather than direct evidence of complete recovery in species composition, vegetation structure, or ecosystem functioning. Accordingly, RI may overestimate ecological recovery when canopy greenness recovers more rapidly than community composition or structural integrity (Iheaturu et al., 2026; Konduri et al., 2023), and may underestimate ecological recovery when ecologically meaningful changes (e.g., below-canopy regeneration or soil-related recovery processes) are weakly expressed in NBR (Kadakci Koca et al., 2024; Pilon et al., 2021). In forests in particular, post-fire vegetation can differ markedly from the original community in composition, structure and function (Durigan and Ratter, 2016; Maezumi et al., 2018; Mesquita et al., 2015). In some Cerrado vegetation types, post-fire spectral greenness may rise rapidly in the short term due to grass and shrub regrowth, but this may reflect a shift to an alternative functional state rather than recovery of the original vegetation state (Durigan, 2025; Konduri et al., 2023; Santos et al., 2025).

4.4. Conservation, policy and future considerations

Building on the spatio-temporal hotspot patterns and protection analyses presented above, our results point to a clear mismatch between disturbance pressure and formal protection across the CAT. Many of the most frequently disturbed frontiers remain weakly represented in the current protected-area network, constituting a protection gap in a high-disturbance landscape. For instance, in Mato Grosso frontier municipalities such as Nova Ubiratã, Nova Maringá, Feliz Natal and Marcelândia as major pressure centres, indicating administratively specific localities where protection and enforcement remain uneven. Previous independent monitoring of illegal logging has also confirmed this (Imazon, 2024). Protection effectiveness can also be contested in high-pressure areas, as illustrated by recent legal and political challenges affecting the Cristalino protected-area complex in northern Mato Grosso (Associated Press, 2022). In this context, our spatially explicit maps provide a practical basis for territorial prioritisation to target frontier belts for the creation or expansion of protected areas and Indigenous territories, and to guide the placement of ecological corridors linking remaining forest and savanna blocks.

Fire emerges as a central driver of persistent degradation in both Amazon forest and Cerrado vegetation. In already disturbed landscapes, recurrent burning is not simply followed by rapid return to pre-disturbance conditions. Instead, it can reinforce long-term reductions in resilience, favour more grass-dominated states, and increase the risk of biome shifts (Brando et al., 2014; Silvério et al., 2013). Our maps of recurrent fire and low RI values highlight priority hotspots where stricter fire control, the adoption of alternative land-use practices and targeted enforcement of anti-burning regulations should be prioritised. At the same time, integrating local and Indigenous knowledge into fire management (Mistry et al., 2005) will be essential to reconcile traditional practices with emerging climatic and disturbance regimes.

The widespread pattern of incomplete recovery also raises concerns for climate mitigation and restoration agendas. Repeated disturbances and slow recovery imply sustained losses of biomass and carbon stocks (Fawcett et al., 2023), as well as potential feedbacks to regional climate through altered surface energy balance and evapotranspiration (Spracklen and Garcia-Carreras, 2015). Areas with a history of recurrent fire and persistently low recovery values should therefore be treated as priority areas for active restoration, rather than relying solely on passive regeneration (Holl and Aide, 2011). Our disturbance and recovery trajectories can help identify where restoration efforts are most urgently needed and where they are more likely to succeed, complementing national restoration commitments and initiatives aimed at reducing emissions from deforestation and forest degradation.

Although our analysis focuses on the Brazilian Cerrado–Amazon Transition, the framework we propose, combining multi-decadal Landsat time series, disturbance segmentation and trajectory-based recovery metrics, is applicable to other tropical deforestation frontiers and ecotones worldwide. Applying similar approaches to regions such as the southern Amazon, the Chaco or the Miombo woodlands could help identify disturbance hotspots, resilience breakdowns and protection gaps in other rapidly changing landscapes. In this sense, our study not only documents the erosion of ecosystem resilience in a single ecotone, but also provides a transferable tool to support conservation planning under accelerating land-use and climate change.

From a technical perspective, our use of 1D-ResNet for disturbance classification showed robust performance across our study region. However, deep learning models typically require relatively large and well-balanced training datasets thus future research could more explicitly examine the sensitivity of disturbance-type classification outcomes to model choice by comparing classification approaches across varying data-availability scenarios.

More broadly, the delineation of forest–savanna transition zones often benefit from integrating multiple ecological indicators rather than relying on a single spatial definition, given that such zones represent gradual shifts in vegetation structure, climate conditions and disturbance regimes. In this study, the spatial extent of the CAT was defined based on the distribution of long-term ecological monitoring plots, providing an empirically grounded representation of the ecotone. Nevertheless, estimates of disturbance extent, hotspot patterns and conservation gaps may remain partially sensitive to boundary specification. Future work could refine transition-zone delineation by integrating additional environmental and structural indicators and by assessing how alternative boundary definitions influence regional disturbance statistics across ecotonal landscapes.

Although our analysis focuses on the Brazilian CAT, the approach presented here demonstrates the broader value of linking long-term disturbance histories with recovery dynamics to support spatially-targeted conservation and restoration planning across ecotones facing accelerating land-use and climate change.

5. Conclusions

The CAT region is a vital ecological zone in the tropics, characterized by frequent agricultural activities. Historically, there has been a significant gap in understanding the dynamics of vegetation disturbances in this area, at least in part due to the difficulty of detecting and identifying specific types of disturbance events across this spatially complex environment. This study provides the first regional-scale integration of LandTrendr temporal segmentation and deep learning-based classification (ResNet), offering a novel framework to investigate the spatio-temporal dynamics of vegetation disturbances in the CAT over the past 35 years. By distinguishing disturbance categories and evaluating their temporal trajectories, our analysis sheds light on the divergent responses of Amazon forest and Cerrado vegetation to disturbance events across the CAT. Our findings indicate that between 1986 and 2020, the CAT region experienced disturbances covering more than 493,000 km^2. Amazon forest clear-cutting emerged as the most prevalent disturbance type (35%), but clear-cutting activities in the Cerrado vegetation accounted for 20% of the detected disturbance events. Whilst Amazon forest disturbances tend to be more concentrated, often representing encroachments into the natural boundaries of the Amazon forest, the Cerrado vegetation is undergoing severe fragmentation often driven by agricultural activities, which result in long-term vegetation loss. In addition, fires, though less destructive in the short term, often prevent full recovery in the long term, particularly in the fire-adapted yet increasingly vulnerable Cerrado vegetation.

Our findings offer valuable insights for future ecological conservation and management efforts in the CAT and underscore the critical importance of protecting these key transitional ecoregions in the context of global climate change. By identifying areas with high disturbance frequencies and ecological vulnerabilities, we can more effectively formulate conservation strategies, optimize resource allocation, and enhance the resilience and adaptive capacity of ecosystems.

CRediT authorship contribution statement

Chuanze Li: Writing – review & editing, Writing – original draft, Visualization, Validation, Software, Methodology, Formal analysis, Data curation, Conceptualization. **Angela Harris:** Writing – review & editing, Supervision, Methodology, Conceptualization. **Beatriz Schwantes Marimon:** Writing – review & editing, Validation, Resources. **Ben Hur Marimon Junior:** Writing – review & editing, Validation, Resources. **Matthew Dennis:** Writing – review & editing, Supervision. **Ricardo Dalagnol:** Writing – review & editing. **Polyanna da Conceição Bispo:** Writing – review & editing, Supervision, Resources, Methodology, Conceptualization.

Funding

This research did not receive any specific grant from funding agencies in the public, commercial, or not-for-profit sectors.

Declaration of competing interest

All authors declare that they have no conflicts of interest.

Appendix A

A sensitivity analysis was conducted using four LandTrendr parameter configurations across three representative vegetation environments (Fig. A1). Three subregions (each 50 km^2) were selected along the major vegetation gradient of the study area, and 50 reference sample points were randomly generated within each subregion to evaluate disturbance detection performance under different parameter settings. Overall results show that the selected configuration (S3) achieved the highest agreement with reference disturbance among all parameter sets (Table A2). The default configuration (S1) showed clear underestimation of disturbance frequency, while the sensitive configuration (S4) increased commission errors due to enhanced detection of short-term spectral variability.

Across subregions, S3 consistently provided stable performance in both Amazon forest-dominated and Cerrado-dominated environments, whereas S4 produced slightly higher accuracy in the mixed Amazon forest–Cerrado landscape but with increased overestimation errors (Table A3). These results indicate that S3 represents the most balanced parameter configuration for disturbance detection across heterogeneous vegetation conditions.

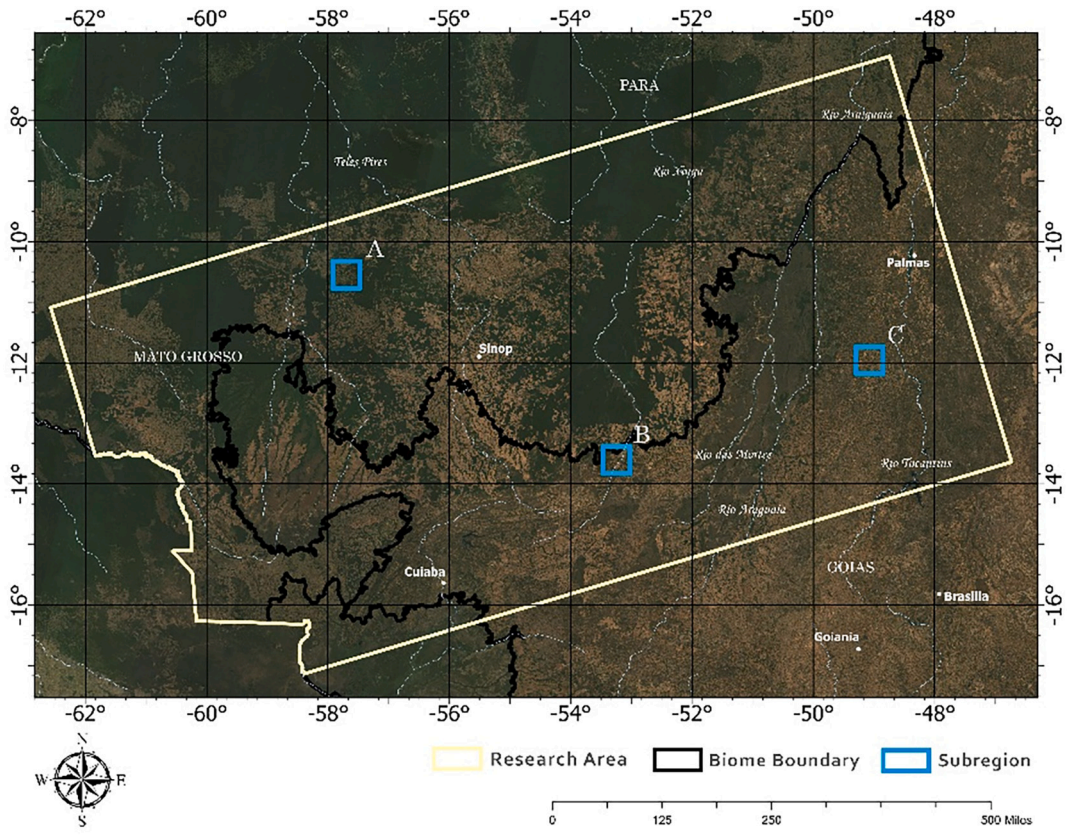

Fig. A1. Locations of the three subregions within the study area used for LandTrendr parameter sensitivity analysis. Subregions A–C represent (A) Amazon forest-dominated landscape, (B) mixed Amazon forest and Cerrado landscape, and (C) Cerrado-dominated landscape.

Table A1
Parameter configurations used for the LandTrendr sensitivity analysis. Four parameter sets were designed to represent default (S1), conservative (S2), selected (S3), and sensitive (S4) configurations by varying maxSegments, recoveryThreshold, and spikeThreshold. These settings were used to evaluate the robustness of disturbance detection results under different segmentation complexity and noise-filtering conditions.

Set	maxSegments	recoveryThreshold	spikeThreshold	Description
S1	6	0.25	0.9	Default configuration commonly used in LT. This setting allows rapid recovery segments and limited segmentation complexity.
S2	8	0.5	0.85	Conservative configuration designed to suppress short-term spectral fluctuations and reduce false disturbance detections. It increases segmentation flexibility while maintaining stronger noise filtering.
S3	9	0.75	0.75	The selected parameter set balances disturbance sensitivity and robustness to noise by allowing sufficient segmentation while restricting rapid recovery artefacts.
S4	10	0.75	0.9	Sensitive configuration allowing more segmentation and weaker spike filtering to capture subtle disturbance signals.

Table A2
Overall accuracy and error-direction comparison of disturbance detection results across four LandTrendr parameter configurations. Accuracy indicates the proportion of sample points where detected disturbance matched reference observations. Underestimation and overestimation represent omission and commission relative to the reference disturbance.

Set	Accuracy	MAE	RMSE	Underestimation	Overestimation	Correct
S1	0.73	0.33	0.67	40	1	109
S2	0.77	0.27	0.58	29	6	115
S3	0.82	0.21	0.51	19	8	123
S4	0.75	0.27	0.57	11	26	113

Table A3
Regional accuracy comparison of disturbance detection performance across different vegetation environments.

Region	Set	Accuracy	MAE	Underestimation	Overestimation
A	S1	0.78	0.28	11	0
A	S2	0.82	0.22	8	1
A	S3	0.84	0.18	5	3
A	S4	0.70	0.32	5	10
B	S1	0.64	0.46	17	1
B	S2	0.66	0.40	12	5
B	S3	0.76	0.30	7	5
B	S4	0.82	0.22	2	7
C	S1	0.76	0.24	12	0
C	S2	0.82	0.18	9	0
C	S3	0.86	0.14	7	0
C	S4	0.74	0.28	4	9

Appendix B

Table B1
Proportion of pixels affected by different number of disturbances across the CAT.

Number of disturbances	% of disturbed pixels
1	100%
2	20.2%
3	2.9%
>3	0.2%

Appendix C

Table C1
Confusion matrix (counts) of the 20% validation dataset used for model development.

		Reference					F1 score
		Amazon forest clear-cutting	Cerrado clear-cutting	Amazon forest fire	Cerrado fire	User's accuracy	
Predicted	Amazon forest clear-cutting	399	11	3	8	95%	96%
	Cerrado clear-cutting	3	381	0	10	97%	95%
	Amazon forest fire	5	0	383	7	97%	98%
	Cerrado Fire	3	18	4	365	94%	94%
	Producer's accuracy	97%	93%	98%	94%		
	Total accuracy	95%					
	Macro-F1	96%					

Data availability

Data will be made available on request.

References

Alencar, A., Nepstad, D., Diaz, M.C.V., 2006. Forest understory fire in the Brazilian Amazon in ENSO and non-ENSO years: area burned and committed carbon emissions. Earth Interact. 10, 1–17. https://doi.org/10.1175/EI150.1.

Alencar, A., Asner, G.P., Knapp, D., Zarin, D., 2011. Temporal variability of forest fires in eastern Amazonia. Ecol. Appl. 21, 2397–2412. https://doi.org/10.1890/10-1168.1.

Alencar, A., Shimbo, J.Z., Lenti, F., Marques, C.B., Zimbres, B., Rosa, M., Arruda, V., Castro, I., Ribeiro, J.P.F.M., Varela, V., Alencar, I., Piontekowski, V., Ribeiro, V., Bustamante, M.M.C., Sano, E.E., Barroso, M., 2020. Mapping three decades of changes in the Brazilian savanna native vegetation using Landsat data processed in the Google Earth Engine platform. Remote Sens. 12. https://doi.org/10.3390/rs12060924.

de Alencar, Ferreira, Mendes, B.T., Pinheiro, M.R., Barretto, E.H.P., Barreiros, A.M., Correia Furquim, S.A., Junqueira Villela, F.N., 2023. Impacts of slash-and-burn cultivation on the soil and vegetation of the Atlantic forest in southeastern Brazil. Hum. Ecol. 51, 655–669. https://doi.org/10.1007/s10745-023-00429-6.

Almeida, D., André, M., Scariot, E.C., Fushita, A.T., dos Santos, J.E., Bogaert, J., 2018. Temporal change of Distance to Nature index for anthropogenic influence monitoring in a protected area and its buffer zone. Ecol. Indic. 91, 189–194. https://doi.org/10.1016/j.ecolind.2018.03.055.

Almeida de Souza, A., Galvão, L.S., Korting, T.S., Prieto, J.D., 2020. Dynamics of savanna clearing and land degradation in the newest agricultural frontier in Brazil. GISci. Remote Sens. 57, 965–984. https://doi.org/10.1080/15481603.2020.1835080.

Alvarado, S.T., Fornazari, T., Cóstola, A., Morellato, L.P.C., Silva, T.S.F., 2017. Drivers of fire occurrence in a mountainous Brazilian cerrado savanna: tracking long-term fire regimes using remote sensing. Ecol. Indic. 78, 270–281. https://doi.org/10.1016/j.ecolind.2017.02.037.

Andela, N., Morton, D.C., Giglio, L., Chen, Y., van der Werf, G.R., Kasibhatla, P.S., DeFries, R.S., Collatz, G.J., Hantson, S., Kloster, S., Bachelet, D., Forrest, M., Lasslop, G., Li, F., Mangeon, S., Melton, J.R., Yue, C., Randerson, J.T., 2017. A human-driven decline in global burned area. Science 356, 1356–1362. https://doi.org/10.1126/science.aal4108.

Andreoni, M., Londoño, E., 2019. Amid outrage over Amazon forest fires, many in the Amazon remain defiant [WWW document]. In: The New York Times. URL. https://www.nytimes.com/2019/08/26/world/americas/brazil-amazon-rainforest-fire.html.

Aragão, L.E.O.C., Anderson, L.O., Fonseca, M.G., Rosan, T.M., Vedovato, L.B., Wagner, F. H., Silva, C.V.J., Silva Junior, C.H.L., Arai, E., Aguiar, A.P., Barlow, J., Berenguer, E., Deeter, M.N., Domingues, L.G., Gatti, L., Gloor, M., Malhi, Y., Marengo, J.A.,

Miller, J.B., Phillips, O.L., Saatchi, S., 2018. 21st Century drought-related fires counteract the decline of Amazon deforestation carbon emissions. Nat. Commun. 9, 536. https://doi.org/10.1038/s41467-017-02771-y.
Araújo, I., Marimon, B.S., Scalon, M.C., Fauset, S., Junior, B.H.M., Tiwari, R., Galbraith, D.R., Gloor, M.U., 2021. Trees at the Amazonia-Cerrado transition are approaching high temperature thresholds. Environ. Res. Lett. 16, 034047. https://doi.org/10.1088/1748-9326/abe3b9.
Arroyo-Kalin, M., 2012. Slash-burn-and-churn: landscape history and crop cultivation in pre-Columbian Amazonia. Quat. Int. 249, 4–18. https://doi.org/10.1016/j.quaint.2011.08.004.
Arvor, D., Tritsch, I., Barcellos, C., Jégou, N., Dubreuil, V., 2017. Land use sustainability on the South-Eastern Amazon agricultural frontier: recent progress and the challenges ahead. Appl. Geogr. 80, 86–97. https://doi.org/10.1016/j.apgeog.2017.02.003.
Associated Press, 2022. A Brazil Court Reopens the Case of a Rainforest Park Larger Than New York City.
Attri, V., Dhiman, R., Sarvade, S., 2020. A review on status, implications and recent trends of forest fire management. Arch. Agric. Environ. Sci. 5, 592–602. https://doi.org/10.26832/24566632.2020.0504024.
Avery, T.E., Berlin, G.L., 1992. Fundamentals of Remote Sensing and Airphoto Interpretation, 5th ed. Macmillan: Maxwell Macmillan International and Maxwell Macmillan Canada.
Bacha, C.J.C., Vinicios de Carvalho, L., 2014. What Explains the Intensification and Diversification of Brazil's Agricultural Production and Exports from 1990 to 2012? https://doi.org/10.2139/ssrn.2470995.
Balch, J.K., Nepstad, D.C., Curran, L.M., Brando, P.M., Portela, O., Guilherme, P., Reuning-Scherer, J.D., de Carvalho, O., 2011. Size, species, and fire behavior predict tree and liana mortality from experimental burns in the Brazilian Amazon. For. Ecol. Manag. 261, 68–77. https://doi.org/10.1016/j.foreco.2010.09.029.
Banskota, A., Kayastha, N., Falkowski, M.J., Wulder, M.A., Froese, R.E., White, J.C., 2014. Forest monitoring using Landsat time series data: a review. Can. J. Remote. Sens. 40, 362–384. https://doi.org/10.1080/07038992.2014.987376.
Barreto, P. (Ed.), 2006. Human Pressure on the Brazilian Amazon Forests, WRI Report. World Resources Institute, Washington, D.C.
Bendini, H.N., Fonseca, L.M.G., Matosak, B.M., Mariano, R.F., Haidar, R.F., Valeriano, D. M., 2022. Evaluating the separability between dry tropical forests and savanna woodlands in the Brazilian savanna using Landsat dense image time series and artificial intelligence. Int. Arch. Photogramm. Remote. Sens. Spat. Inf. Sci. 43, 841–847. https://doi.org/10.5194/isprs-archives-XLIII-B3-2022-841-2022.
Bonini, I., Hur Marimon-Junior, B., Matricardi, E., Phillips, O., Petter, F., Oliveira, B., Marimon, B.S., 2018. Collapse of ecosystem carbon stocks due to forest conversion to soybean plantations at the Amazon-Cerrado transition. For. Ecol. Manag. 414, 64–73. https://doi.org/10.1016/j.foreco.2018.01.038.
Brando, P.M., Balch, J.K., Nepstad, D.C., Morton, D.C., Putz, F.E., Coe, M.T., Silvério, D., Macedo, M.N., Davidson, E.A., Nóbrega, C.C., Alencar, A., Soares-Filho, B.S., 2014. Abrupt increases in Amazonian tree mortality due to drought–fire interactions. Proc. Natl. Acad. Sci. 111, 6347–6352. https://doi.org/10.1073/pnas.1305499111.
Bright, B.C., Hudak, A.T., Kennedy, R.E., Braaten, J.D., Henareh Khalyani, A., 2019. Examining post-fire vegetation recovery with Landsat time series analysis in three western North American forest types. Fire Ecol. 15, 8. https://doi.org/10.1186/s42408-018-0021-9.
Bullock, E.L., Woodcock, C.E., 2021. Carbon loss and removal due to forest disturbance and regeneration in the Amazon. Sci. Total Environ. 764, 142839. https://doi.org/10.1016/j.scitotenv.2020.142839.
Carneiro, B.M., de Carvalho Junior, O.A., Guimarães, R.F., Evangelista, B.A., de Carvalho, O.L.F., 2024. Exploiting legal reserve compensation as a mechanism for unlawful deforestation in the Brazilian Cerrado biome, 2012–2022. Sustainability 16, 9557. https://doi.org/10.3390/su16219557.
Cerri, C.E.P., Cerri, C.C., Maia, S.M.F., Cherubin, M.R., Feigl, B.J., Lal, R., 2018. Reducing Amazon deforestation through agricultural intensification in the Cerrado for advancing food security and mitigating climate change. Sustainability 10, 989. https://doi.org/10.3390/su10040989.
Chen, Xi, Zhao, W., Chen, J., Qu, Y., Wu, D., Chen, Xuehong, 2021. Mapping large-scale forest disturbance types with multi-temporal CNN framework. Remote Sens. 13, 5177. https://doi.org/10.3390/rs13245177.
Cochran, W.G., 1977. Sampling Techniques. John Wiley & Sons.
Coe, M.T., Marthews, T.R., Costa, M.H., Galbraith, D.R., Greenglass, N.L., Imbuzeiro, H. M.A., Levine, N.M., Malhi, Y., Moorcroft, P.R., Muza, M.N., Powell, T.L., Saleska, S. R., Solorzano, L.A., Wang, J., 2013. Deforestation and climate feedbacks threaten the ecological integrity of south–southeastern Amazonia. Philos. Trans. R. Soc. B Biol. Sci. 368, 20120155. https://doi.org/10.1098/rstb.2012.0155.
Cohen, W.B., Yang, Z., Kennedy, R., 2010. Detecting trends in forest disturbance and recovery using yearly Landsat time series: 2. TimeSync — tools for calibration and validation. Remote Sens. Environ. 114, 2911–2924. https://doi.org/10.1016/j.rse.2010.07.010.
Colman, C.B., Guerra, A., Almagro, A., de Oliveira Roque, F., Rosa, I.M., Fernandes, G. W., Oliveira, P.T.S., 2024. Modeling the Brazilian Cerrado land use change highlights the need to account for private property sizes for biodiversity conservation. Sci. Rep. 14, 4559. https://doi.org/10.1038/s41598-024-55207-1.
Connell, J.H., Slatyer, R.O., 1977. Mechanisms of succession in natural communities and their role in community stability and organization. Am. Nat. 111, 1119–1144. https://doi.org/10.1086/283241.
Crist, E.P., Cicone, R.C., 1984. A physically-based transformation of Thematic Mapper data—the TM Tasseled Cap. IEEE Trans. Geosci. Remote Sens. GE-22, 256–263. https://doi.org/10.1109/TGRS.1984.350619.
da Cruz Silva, A., Veenendaal, E., Van der Plas, F., de Oliveira Júnior, V.D., do Vale, V.S., Meira-Neto, J.A.A., 2025. Vegetation transition in the central Brazilian Cerrado is better explained by structure than tree composition differences. Plant Ecol. 226, 563–572. https://doi.org/10.1007/s11258-025-01500-6.
Da Veiga, R.M., Von Randow, C., Burton, C., Kelley, D.I., Cardoso, M., Morelli, F., 2025. Fire emissions in the Brazilian Cerrado — dynamics, estimates, management, and their role in the global carbon budget. Nat. Hazards Earth Syst. Sci. 25, 3581–3601. https://doi.org/10.5194/nhess-25-3581-2025.
Dalagnol, R., Wagner, F.H., Galvão, L.S., Braga, D., Osborn, F., Sagang, L.B., da Conceição Bispo, P., Payne, M., Junior, C.S., Favrichon, S., 2023. Mapping tropical forest degradation with deep learning and Planet NICFI data. Remote Sens. Environ. 298, 113798. https://doi.org/10.1016/j.rse.2023.113798.
De Faria, B.L., Marano, G., Piponiot, C., Silva, C.A., Dantas, V. de L., Rattis, L., Rech, A.R., Collalti, A., 2021a. Model-based estimation of Amazonian forests recovery time after drought and fire events. Forests 12, 8. https://doi.org/10.3390/f12010008.
De Faria, B.L., Staal, A., Silva, C.A., Martin, P.A., Panday, P.K., Dantas, V.L., 2021b. Climate change and deforestation increase the vulnerability of Amazonian forests to post-fire grass invasion. Glob. Ecol. Biogeogr. 30, 2368–2381. https://doi.org/10.1111/geb.13388.
De Marco Jr., P., de Souza, R.A., Andrade, F.A., Villén-Pérez, S., Nóbrega, C.C., Campello, L.M., Caldas, M., 2023. The value of private properties for the conservation of biodiversity in the Brazilian Cerrado. Science 380, 298–301. https://doi.org/10.1126/science.abq7768.
DeVries, B., Decuyper, M., Verbesselt, J., Zeileis, A., Herold, M., Joseph, S., 2015. Tracking disturbance-regrowth dynamics in tropical forests using structural change detection and Landsat time series. Remote Sens. Environ. 169, 320–334. https://doi.org/10.1016/j.rse.2015.08.020.
Dionizio, E.A., Costa, M.H., 2019. Influence of land use and land cover on hydraulic and physical soil properties at the Cerrado agricultural frontier. Agriculture 9, 24. https://doi.org/10.3390/agriculture9010024.
Dormann, C.F., Bagnara, M., Boch, S., Hinderling, J., Janeiro-Otero, A., Schäfer, D., Schall, P., Hartig, F., 2020. Plant species richness increases with light availability, but not variability, in temperate forests understorey. BMC Ecol. 20, 1–9. https://doi.org/10.1186/s12898-020-00311-9.
Drüke, M., Sakschewski, B., von Bloh, W., Billing, M., Lucht, W., Thonicke, K., 2023. Fire may prevent future Amazon forest recovery after large-scale deforestation. Commun. Earth Environ. 4, 248. https://doi.org/10.1038/s43247-023-00911-5.
Durigan, G., 2025. Cerrado: biodiversity and ecosystem services under severe threat by misguided restoration. Ann. Bot., mcaf306 https://doi.org/10.1093/aob/mcaf306.
Durigan, G., Ratter, J.A., 2016. The need for a consistent fire policy for Cerrado conservation. J. Appl. Ecol. 53, 11–15. https://doi.org/10.1111/1365-2664.12559.
eMapR Lab, 2018. T-GEE guide [WWW Document]. In: LT-GEE Guide. URL. https://emapr.github.io/LT-GEE/ui-applications.html (accessed 2.24.26).
Epting, J., Verbyla, D., Sorbel, B., 2005. Evaluation of remotely sensed indices for assessing burn severity in interior Alaska using Landsat™ and ETM^{+}. Remote Sens. Environ. 96, 328–339. https://doi.org/10.1016/j.rse.2005.03.002.
De Faria, L.D., Matricardi, E.A.T., Marimon, B.S., Miguel, E.P., Junior, B.H.M., de Oliveira, E.A., Prestes, N.C.C.S., de Carvalho, O.L.F., 2024. Biomass prediction using Sentinel-2 imagery and an artificial neural network in the Amazon/Cerrado transition region. Forests 15, 1599. https://doi.org/10.3390/f15091599.
Fawcett, D., Sitch, S., Ciais, P., Wigneron, J.P., Silva-Junior, C.H.L., Heinrich, V., Vancutsem, C., Achard, F., Bastos, A., Yang, H., Li, X., Albergel, C., Friedlingstein, P., Aragão, L.E.O.C., 2023. Declining Amazon biomass due to deforestation and subsequent degradation losses exceeding gains. Glob. Chang. Biol. 29, 1106–1118. https://doi.org/10.1111/gcb.16513.
Fearnside, P.M., 2005. Deforestation in Brazilian Amazonia: history, rates, and consequences. Conserv. Biol. 19, 680–688. https://doi.org/10.1111/j.1523-1739.2005.00697.x.
Flores, B.M., Holmgren, M., 2021. Why forest fails to recover after repeated wildfires in Amazonian floodplains? Experimental evidence on tree recruitment limitation. J. Ecol. 109, 3473–3486. https://doi.org/10.1111/1365-2745.13769.
Flores, B.M., Montoya, E., Sakschewski, B., Nascimento, N., Staal, A., Betts, R.A., Levis, C., Lapola, D.M., Esquível-Muelbert, A., Jakovac, C., 2024. Critical transitions in the Amazon forest system. Nature 626, 555–564. https://doi.org/10.1038/s41586-023-06970-0.
Gao, B., 1996. NDWI—a normalized difference water index for remote sensing of vegetation liquid water from space. Remote Sens. Environ. 58, 257–266. https://doi.org/10.1016/S0034-4257(96)00067-3.
Golin, T., 2024. The southern grasslands and the expropriation of indigenous territories. In: Overbeck, G.E., Pillar, V.D.P., Müller, S.C., Bencke, G.A. (Eds.), South Brazilian Grasslands. Springer, Cham, pp. 145–174. https://doi.org/10.1007/978-3-031-42580-6_7.
Gomes, L., Simões, S.J.C., Dalla Nora, E.L., de Sousa-Neto, E.R., Forti, M.C., Ometto, J.P. H.B., 2019. Agricultural expansion in the Brazilian Cerrado: increased soil and nutrient losses and decreased agricultural productivity. Land 8, 12. https://doi.org/10.3390/land8010012.
Gómez, C., White, J.C., Wulder, M.A., 2011. Characterizing the state and processes of change in a dynamic forest environment using hierarchical spatio-temporal segmentation. Remote Sens. Environ. 115, 1665–1679. https://doi.org/10.1016/j.rse.2011.02.025.
Gonçalves, R.V.S., Cardoso, J.C.F., Oliveira, P.E., Oliveira, D.C., 2021. Changes in the Cerrado vegetation structure: insights from more than three decades of ecological succession. Web Ecol. 21, 55–64. https://doi.org/10.5194/we-21-55-2021.
Gorelick, N., Hancher, M., Dixon, M., Ilyushchenko, S., Thau, D., Moore, R., 2017. Google Earth Engine: planetary-scale geospatial analysis for everyone. Remote Sens. Environ. 202, 18–27. https://doi.org/10.1016/j.rse.2017.06.031.

Greenberg, C., 2026. The Amazon — And Our Future — Is Being Burned for Profit [WWW document]. Greenpeace International. URL. https://www.greenpeace.org/international/story/55533/amazon-rainforest-fires-2022-brazil-causes-climate/ (accessed 2.23.26).

Gunderson, L.H., 2000. Ecological resilience—in theory and application. Annu. Rev. Ecol. Evol. Syst. 31, 425–439. https://doi.org/10.1146/annurev.ecolsys.31.1.425.

Guo, J., Li, Q., Xie, H., Li, J., Qiao, L., Zhang, C., Yang, G., Wang, F., 2022. Monitoring of vegetation disturbance and restoration at the dumping sites of the baorixile open-pit mine based on the LandTrendr algorithm. Int. J. Environ. Res. Public Health 19, 9066. https://doi.org/10.3390/ijerph19159066.

Hansen, M.C., Potapov, P.V., Moore, R., Hancher, M., Turubanova, S.A., Tyukavina, A., Thau, D., Stehman, S.V., Goetz, S.J., Loveland, T.R., Kommareddy, A., Egorov, A., Chini, L., Justice, C.O., Townshend, J.R.G., 2013. High-resolution global maps of 21st-century forest cover change. Science 342, 850–853. https://doi.org/10.1126/science.1244693.

Hansen, M.C., Krylov, A., Tyukavina, A., Potapov, P.V., Turubanova, S., Zutta, B., Ifo, S., Margono, B., Stolle, F., Moore, R., 2016. Humid tropical forest disturbance alerts using Landsat data. Environ. Res. Lett. 11, 034008. https://doi.org/10.1088/1748-9326/11/3/034008.

Harding, T., Herzberg, J., Kuralbayeva, K., 2021. Commodity prices and robust environmental regulation: evidence from deforestation in Brazil. J. Environ. Econ. Manag. 108, 102452. https://doi.org/10.1016/j.jeem.2021.102452.

He, K., Zhang, X., Ren, S., Sun, J., 2015. Deep Residual Learning for Image Recognition. https://doi.org/10.48550/arXiv.1512.03385.

He, K., Zhang, X., Ren, S., Sun, J., 2016. Deep residual learning for image recognition, In: 2016 IEEE Conference on Computer Vision and Pattern Recognition (CVPR). Presented at the 2016 IEEE Conference on Computer Vision and Pattern Recognition (CVPR), IEEE, Las Vegas, NV, USA, pp. 770–778. doi:https://doi.org/10.1109/CVPR.2016.90.

Healey, S.P., Yang, Z., Cohen, W.B., Pierce, D.J., 2006. Application of two regression-based methods to estimate the effects of partial harvest on forest structure using Landsat data. Remote Sens. Environ. 101, 115–126. https://doi.org/10.1016/j.rse.2005.12.006.

Hirota, M., Holmgren, M., Van Nes, E.H., Scheffer, M., 2011. Global resilience of tropical forest and savanna to critical transitions. Science 334, 232–235. https://doi.org/10.1126/science.1210657.

Hislop, S., Jones, S., Soto-Berelov, M., Skidmore, A., Haywood, A., Nguyen, T.H., 2018. Using Landsat spectral indices in time-series to assess wildfire disturbance and recovery. Remote Sens. 10. https://doi.org/10.3390/rs10030460.

Hoffmann, W.A., 2005. Ecologia comparativa de espécies lenhosas de cerrado e de mata. In: Cerrado: Ecologia, Biodiversidade e Conservação. Ministério do Meio Ambiente, Brasília, DF, pp. 157–165.

Hoffmann, W.A., Geiger, E.L., Gotsch, S.G., Rossatto, D.R., Silva, L.C.R., Lau, O.L., Haridasan, M., Franco, A.C., 2012. Ecological thresholds at the savanna-forest boundary: how plant traits, resources and fire govern the distribution of tropical biomes. Ecol. Lett. 15, 759–768. https://doi.org/10.1111/j.1461-0248.2012.01789.x.

Holl, K.D., Aide, T.M., 2011. When and where to actively restore ecosystems? For. Ecol. Manag. 261, 1558–1563. https://doi.org/10.1016/j.foreco.2010.07.004.

Holling, C.S., 1973. Resilience and stability of ecological systems. Annu. Rev. Ecol. Evol. Syst. 4, 1–23. https://doi.org/10.1146/annurev.es.04.110173.000245.

IBGE, 2019. Biomas e Sistema Costeiro-Marinho do Brasil.

Iheaturu, C.J., Curatola Fernández, G.F., Wingate, V.R., Akinyemi, F.O., Okolie, C.J., Ifejika Speranza, C., 2026. Remote sensing of tropical forest recovery: a review and decision-support framework for multi-sensor integration. Remote Sens. Environ. 335, 115257. https://doi.org/10.1016/j.rse.2026.115257.

Imazon, 2024. Timber Harvesting Monitoring System (Simex): Mapping of logging in Mato Grosso State (August 2022 to July 2023). Instituto do Homem e Meio Ambiente da Amazônia (Imazon), Brazil.

Kadakci Koca, T., Küçükuysal, C., Gül, M., Esetlili, T., 2024. A comprehensive approach to soil burn severity mapping for erosion susceptibility assessment. CATENA 245, 108302. https://doi.org/10.1016/j.catena.2024.108302.

Kennedy, R.E., Yang, Z., Cohen, W.B., 2010. Detecting trends in forest disturbance and recovery using yearly Landsat time series: 1. LandTrendr — temporal segmentation algorithms. Remote Sens. Environ. 114, 2897–2910. https://doi.org/10.1016/j.rse.2010.07.008.

Kennedy, R.E., Yang, Z., Cohen, W.B., Pfaff, E., Braaten, J., Nelson, P., 2012. Spatial and temporal patterns of forest disturbance and regrowth within the area of the Northwest Forest Plan. Remote Sens. Environ. 122, 117–133. https://doi.org/10.1016/j.rse.2011.09.024.

Kennedy, R.E., Yang, Z., Gorelick, N., Braaten, J., Cavalcante, L., Cohen, W.B., Healey, S., 2018. Implementation of the LandTrendr algorithm on Google Earth Engine. Remote Sens. 10, 691. https://doi.org/10.3390/rs10050691.

Key, C.H., 2006. Ecological and sampling constraints on defining landscape fire severity. Fire Ecol. 2, 34–59. https://doi.org/10.4996/fireecology.0202034.

Key, C.H., Benson, N.C., 2006. Landscape assessment (LA). In: FIREMON: fire effects monitoring and inventory system. Gen. Tech. Rep. RMRS-GTR-164-CD. US Department of Agriculture, Forest Service, Rocky Mountain Research Station, Fort Collins, CO. https://doi.org/10.2737/RMRS-GTR-164.

Konduri, V.S., Morton, D.C., Andela, N., 2023. Tracking changes in vegetation structure following fire in the Cerrado biome using ICESat-2. JGR Biogeosci. 128. https://doi.org/10.1029/2022JG007046 e2022JG007046.

Koonce, B., 2021. ResNet 50. In: Koonce, B. (Ed.), Convolutional Neural Networks with Swift for Tensorflow: Image Recognition and Dataset Categorization. Apress, Berkeley, CA, pp. 63–72. https://doi.org/10.1007/978-1-4842-6168-2_6.

Lenza, E., Santos, J.O., Maracahipes-Santos, L., 2015. Species composition, diversity, and vegetation structure in a gallery forest-*cerrado sensu stricto* transition zone in eastern Mato Grosso, Brazil. Acta Bot. Bras. 29, 327–338. https://doi.org/10.1590/0102-33062014abb3697.

Li, C., Harris, A., Marimon, B.S., Marimon Junior, B.H., Dennis, M., Bispo, P. da C., 2025. Mapping the Cerrado–Amazon transition using PlanetScope–Sentinel data fusion and a U-Net deep learning framework. Remote Sens. 17, 2138. https://doi.org/10.3390/rs17132138.

Li, K., Zhao, W., Chen, J., Zhang, L., Hu, D., Wang, Q., 2023. Predicting crop growth patterns with spatial–temporal deep feature exploration for early mapping. Remote Sens. 15. https://doi.org/10.3390/rs15133285.

Lucas, K.R.G., Caldarelli, C.E., Ventura, M.U., 2023. Agriculture and biodiversity damage: a prospective evaluation of the impact of Brazilian agriculture on its ecoregions through life cycle assessment methodology. Sci. Total Environ. 899, 165762. https://doi.org/10.1016/j.scitotenv.2023.165762.

Luiz, C.H.P., Steinke, V.A., 2022. Recent environmental legislation in Brazil and the impact on Cerrado deforestation rates. Sustainability 14, 8096. https://doi.org/10.3390/su14138096.

Machida, W.S., Gomes, L., Moser, P., Castro, I.B., Miranda, S.C., da Silva-Júnior, M.C., Bustamante, M.M.C., 2021. Long term post-fire recovery of woody plants in savannas of Central Brazil. For. Ecol. Manag. 493, 119255. https://doi.org/10.1016/j.foreco.2021.119255.

Maezumi, S.Y., Robinson, M., de Souza, J., Urrego, D.H., Schaan, D., Alves, D., Iriarte, J., 2018. New insights from pre-Columbian land use and fire management in Amazonian dark earth forests. Front. Ecol. Evol. 6. https://doi.org/10.3389/fevo.2018.00111.

Maia, S.M.F., Ogle, S.M., Cerri, C.E.P., Cerri, C.C., 2010. Soil organic carbon stock change due to land use activity along the agricultural frontier of the southwestern Amazon, Brazil, between 1970 and 2002. Glob. Chang. Biol. 16, 2775–2788. https://doi.org/10.1111/j.1365-2486.2009.02105.x.

Maracahipes, L., Marimon, B., Lenza, E., Marimon-Junior, B.H., Almeida de Oliveira, E., Mews, H., Gomes, L., Feldpausch, T., 2014. Post-fire dynamics of woody vegetation in seasonally flooded forests (impucas) in the Cerrado-Amazonian Forest transition zone. Flora: Morphol. Distrib. Funct. Ecol. Plants 209. https://doi.org/10.1016/j.flora.2014.02.008.

Maracahipes-Santos, L., Lenza, E., dos Santos, J.O., Marimon, B.S., Eisenlohr, P.V., Marimon Junior, B.H., Feldpausch, T.R., 2015. Diversity, floristic composition, and structure of the woody vegetation of the Cerrado in the Cerrado–Amazon transition zone in Mato Grosso, Brazil. Braz. J. Bot. 38, 877–887. https://doi.org/10.1007/s40415-015-0186-2.

Marengo, J.A., Nobre, C.A., Tomasella, J., Oyama, M.D., de Oliveira, G.S., de Oliveira, R., Camargo, H., Alves, L.M., Brown, I.F., 2008. The drought of Amazonia in 2005. J. Clim. 21, 495–516. https://doi.org/10.1175/2007JCLI1600.1.

Maretto, R.V., Fonseca, L.M., Jacobs, N., Körting, T.S., Bendini, H.N., Parente, L.L., 2020. Spatio-temporal deep learning approach to map deforestation in Amazon rainforest. IEEE Geosci. Remote Sens. Lett. 18, 771–775. https://doi.org/10.1109/LGRS.2020.2986407.

Marimon, B.S., Lima, E.D.S., Duarte, T.G., Chieregatto, L.C., Ratter, J.A., 2006. Observations on the vegetation of northeastern Mato Grosso, Brazil. IV. An analysis of the Cerrado–Amazonian forest ecotone. Edinb. J. Bot. 63, 323–341. https://doi.org/10.1017/S0960428606000576.

Marimon, B.S., Marimon-Junior, B.H., Feldpausch, T.R., Oliveira-Santos, C., Mews, H.A., Lopez-Gonzalez, G., Lloyd, J., Franczak, D.D., de Oliveira, E.A., Maracahipes, L., Miguel, A., Lenza, E., Phillips, O.L., 2014. Disequilibrium and hyperdynamic tree turnover at the forest–cerrado transition zone in southern Amazonia. Plant Ecol. Divers. 7, 281–292. https://doi.org/10.1080/17550874.2013.818072.

Marimon Junior, B.H., Haridasan, M., 2005. Comparação da vegetação arbórea e características edáficas de um cerradão e um cerrado sensu stricto em áreas adjacentes sobre solo distrófico no leste de Mato Grosso, Brasil. Acta Bot. Bras. 19, 913–926.

Marques, E.Q., Marimon-Junior, B.H., Marimon, B.S., Matricardi, E.A.T., Mews, H.A., Colli, G.R., 2020. Redefining the Cerrado–Amazonia transition: implications for conservation. Biodivers. Conserv. 29, 1501–1517. https://doi.org/10.1007/s10531-019-01720-z.

Marques, E.Q., Silvério, D.V., Galvão, L.S., Aragão, L.E.O.C., Uribe, M.R., Macedo, M.N., Rattis, L., Alencar, A.A.C., Brando, P.M., 2024. Assessing the effectiveness of vegetation indices in detecting forest disturbances in the southeast Amazon. Sci. Rep. 14, 27287. https://doi.org/10.1038/s41598-024-77924-3.

Martello, F., dos Santos, J.S., Silva-Neto, C.M., Cássia-Silva, C., Siqueira, K.N., de Ataíde, M.V.R., Ribeiro, M.C., Collevatti, R.G., 2023. Landscape structure shapes the diversity of plant reproductive traits in agricultural landscapes in the Brazilian Cerrado. Agric. Ecosyst. Environ. 341, 108216. https://doi.org/10.1016/j.agee.2022.108216.

Matricardi, E.A.T., Skole, D.L., Pedlowski, M.A., Chomentowski, W., Fernandes, L.C., 2010. Assessment of tropical forest degradation by selective logging and fire using Landsat imagery. Remote Sens. Environ. 114, 1117–1129. https://doi.org/10.1016/j.rse.2010.01.001.

Matricardi, E.A.T., Skole, D.L., Pedlowski, M.A., Chomentowski, W., 2013. Assessment of forest disturbances by selective logging and forest fires in the Brazilian Amazon using Landsat data. Int. J. Remote Sens. 34, 1057–1086. https://doi.org/10.1080/01431161.2012.717182.

Matricardi, E.A.T., Skole, D.L., Costa, O.B., Pedlowski, M.A., Samek, J.H., Miguel, E.P., 2020. Long-term forest degradation surpasses deforestation in the Brazilian Amazon. Science 369, 1378–1382. https://doi.org/10.1126/science.abb3021.

de Medeiros, M.B., Fiedler, N.C., 2011. Heterogeneidade de ecossistemas, modelos de desequilíbrio e distúrbios. Biodivers. Bras. 1, 4–11. https://doi.org/10.37002/biodiversidadebrasileira.v1i2.135.
Melo, P., Sparacino, J., Argibay, D., Sousa Júnior, V., Barros, R., Espindola, G., 2021. Assessing wildfire regimes in indigenous lands of the Brazilian savannah-like cerrado. Fire 4, 34. https://doi.org/10.3390/fire4030034.
Mesquita, R.C.G., Massoca, P.E. dos S., Jakovac, C.C., Bentos, T.V., Williamson, G.B., 2015. Amazon rain forest succession: stochasticity or land-use legacy? BioScience 65, 849–861. https://doi.org/10.1093/biosci/biv108.
Miettinen, J., Shimabukuro, Y.E., Beuchle, R., Grecchi, R.C., Gomez, M.V., Simonetti, D., Achard, F., 2015. On the extent of fire-induced forest degradation in Mato Grosso, Brazilian Amazon, in 2000, 2005 and 2010. Int. J. Wildland Fire 25, 129–136. https://doi.org/10.1071/WF15036.
Miller, J.D., Thode, A.E., 2007. Quantifying burn severity in a heterogeneous landscape with a relative version of the delta Normalized Burn Ratio (dNBR). Remote Sens. Environ. 109, 66–80. https://doi.org/10.1016/j.rse.2006.12.006.
Miller, J.D., Knapp, E.E., Key, C.H., Skinner, C.N., Isbell, C.J., Creasy, R.M., Sherlock, J. W., 2009. Calibration and validation of the relative differenced Normalized Burn Ratio (RdNBR) to three measures of fire severity in the Sierra Nevada and Klamath Mountains, California, USA. Remote Sens. Environ. 113, 645–656. https://doi.org/10.1016/j.rse.2008.11.009.
Miranda, H.S., Sato, M.N., Neto, W.N., Aires, F.S., 2009. Fires in the cerrado, the Brazilian savanna. In: Cochrane, M.A. (Ed.), Tropical Fire Ecology: Climate Change, Land Use, and Ecosystem Dynamics. Springer, Berlin, Heidelberg, pp. 427–450. https://doi.org/10.1007/978-3-540-77381-8_15.
Mistry, J., Berardi, A., Andrade, V., Krahô, T., Krahô, P., Leonardos, O., 2005. Indigenous fire management in the cerrado of Brazil: the case of the Krahô of Tocantíns. Hum. Ecol. 33, 365–386. https://doi.org/10.1007/s10745-005-4143-8.
Moreira, A.G., 2000. Effects of fire protection on savanna structure in Central Brazil. J. Biogeogr. 27, 1021–1029. https://doi.org/10.1046/j.1365-2699.2000.00422.x.
Moreno-Mateos, D., Barbier, E.B., Jones, P.C., Jones, H.P., Aronson, J., López-López, J.A., McCrackin, M.L., Meli, P., Montoya, D., Rey Benayas, J.M., 2017. Anthropogenic ecosystem disturbance and the recovery debt. Nat. Commun. 8, 14163. https://doi.org/10.1038/ncomms14163.
Morresi, D., Marzano, R., Lingua, E., Motta, R., Garbarino, M., 2022. Mapping burn severity in the western Italian Alps through phenologically coherent reflectance composites derived from Sentinel-2 imagery. Remote Sens. Environ. 269, 112800. https://doi.org/10.1016/j.rse.2021.112800.
Morton, D.C., DeFries, R.S., Shimabukuro, Y.E., Anderson, L.O., Arai, E., del Bon Espirito-Santo, F., Freitas, R., Morisette, J., 2006. Cropland expansion changes deforestation dynamics in the southern Brazilian Amazon. Proc. Natl. Acad. Sci. 103, 14637–14641. https://doi.org/10.1073/pnas.0606377103.
Morton, D.C., Le Page, Y., DeFries, R., Collatz, G.J., Hurtt, G.C., 2013. Understorey fire frequency and the fate of burned forests in southern Amazonia. Philos. Trans. R. Soc. Lond. Ser. B Biol. Sci. 368, 20120163. https://doi.org/10.1098/rstb.2012.0163.
Mota, F.B.S., Ferreira, K.R., Escada, M.I.S., 2024. Evaluating forest disturbance detection methods based on satellite image time series for Amazon deforestation alerts. In: Int. Arch. Photogramm. Remote. Sens. Spat. Inf. Sci. XLVIII-3-2024, pp. 357–364. https://doi.org/10.5194/isprs-archives-XLVIII-3-2024-357-2024.
Myers, N., 2023. Tropical deforestation: rates and patterns. In: The Causes of Tropical Deforestation, pp. 27–40.
Nepstad, D.C., Stickler, C.M., Almeida, O.T., 2006. Globalization of the Amazon soy and beef industries: opportunities for conservation. Conserv. Biol. 20, 1595–1603. https://doi.org/10.1111/j.1523-1739.2006.00510.x.
Ochtyra, A., 2020. Forest disturbances in Polish Tatra Mountains for 1985–2016 in relation to topography, stand features, and protection zone. Forests 11, 579. https://doi.org/10.3390/f11050579.
Oeser, J., Pflugmacher, D., Senf, C., Heurich, M., Hostert, P., 2017. Using intra-annual Landsat time series for attributing forest disturbance agents in Central Europe. Forests 8. https://doi.org/10.3390/f8070251.
de Oliveira, B., Junior, B.H.M., Mews, H.A., Valadao, M.B.X., Marimon, B.S., 2017. Unraveling the ecosystem functions in the Amazonia-Cerrado transition: evidence of hyperdynamic nutrient cycling. Plant Ecol. 218, 225–240. https://doi.org/10.1007/s11258-016-0681-y.
Olofsson, P., Foody, G.M., Herold, M., Stehman, S.V., Woodcock, C.E., Wulder, M.A., 2014. Good practices for estimating area and assessing accuracy of land change. Remote Sens. Environ. 148, 42–57. https://doi.org/10.1016/j.rse.2014.02.015.
Ouma, S., 2020. Farming as Financial Asset: Global Finance and the Making of Institutional Landscapes. Agenda Publishing Limited.
Pellegrini, A.F.A., Ahlström, A., Hobbie, S.E., Reich, P.B., Nieradzik, L.P., Staver, A.C., Scharenbroch, B.C., Jumpponen, A., Anderegg, W.R.L., Randerson, J.T., Jackson, R. B., 2018. Fire frequency drives decadal changes in soil carbon and nitrogen and ecosystem productivity. Nature 553, 194–198. https://doi.org/10.1038/nature24668.
Pelletier, C., Webb, G.I., Petitjean, F., 2019. Temporal convolutional neural network for the classification of satellite image time series. Remote Sens. 11. https://doi.org/10.3390/rs11050523.
Perbet, P., Guindon, L., Côté, J.-F., Béland, M., 2024. Evaluating deep learning methods applied to Landsat time series subsequences to detect and classify boreal forest disturbances events: the challenge of partial and progressive disturbances. Remote Sens. Environ. 306, 114107. https://doi.org/10.1016/j.rse.2024.114107.
Pérez-Cabello, F., Montorio, R., Alves, D.B., 2021. Remote sensing techniques to assess post-fire vegetation recovery. Curr. Opin. Environ. Sci. Health 21, 100251. https://doi.org/10.1016/j.coesh.2021.100251.
Pickell, P.D., Hermosilla, T., Frazier, R.J., Coops, N.C., Wulder, M.A., 2016. Forest recovery trends derived from Landsat time series for North American boreal forests. Int. J. Remote Sens. 37, 138–149. https://doi.org/10.1080/2150704X.2015.1126375.
Pilon, N.A.L., Cava, M.G.B., Hoffmann, W.A., Abreu, R.C.R., Fidelis, A., Durigan, G., 2021. The diversity of post-fire regeneration strategies in the cerrado ground layer. J. Ecol. 109, 154–166. https://doi.org/10.1111/1365-2745.13456.
Pinty, B., Verstraete, M.M., Gobron, N., Roveda, F., Govaerts, Y., 2000. Do man-made fires affect Earth's surface reflectance at continental scales? EOS Trans. Am. Geophys. Union 81, 381–389. https://doi.org/10.1029/00EO00281.
Pivello, V.R., 2011. The use of fire in the Cerrado and Amazonian rainforests of Brazil: past and present. Fire Ecol. 7, 24–39. https://doi.org/10.4996/fireecology.0701024.
Pivello, V.R., Vieira, I., Christianini, A.V., Ribeiro, D.B., da Silva Menezes, L., Berlinck, C. N., Melo, F.P.L., Marengo, J.A., Tornquist, C.G., Tomas, W.M., Overbeck, G.E., 2021. Understanding Brazil's catastrophic fires: causes, consequences and policy needed to prevent future tragedies. Perspect. Ecol. Conserv. 19, 233–255. https://doi.org/10.1016/j.pecon.2021.06.005.
Pokorny, B., Pacheco, P., 2014. Money from and for forests: a critical reflection on the feasibility of market approaches for the conservation of Amazonian forests. J. Rural. Stud. 36, 441–452. https://doi.org/10.1016/j.jrurstud.2014.09.004.
Pokorny, B., Scholz, I., De Jong, W., 2013. REDD+ for the poor or the poor for REDD+? About the limitations of environmental policies in the Amazon and the potential of achieving environmental goals through pro-poor policies. Ecol. Soc. 18. https://www.jstor.org/stable/26269329.
Pokorny, B., Pacheco, P., de Jong, W., Entenmann, S.K., 2021. Forest frontiers out of control: the long-term effects of discourses, policies, and markets on conservation and development of the Brazilian Amazon. Ambio 50, 2199–2223. https://doi.org/10.1007/s13280-021-01637-4.
Projeto RADAMBRASIL, 1981. Folha SD.22 Goiás: Geologia, Geomorfologia, Pedologia, Vegetação, Uso Potencial Da Terra, Levantamento de Recursos Naturais. Ministério das Minas e Energia. Secretaria Geral, Rio de Janeiro, p. 636.
Qiu, D., Liang, Y., Shang, R., Chen, J.M., 2023. Improving LandTrendr forest disturbance mapping in China using multi-season observations and multispectral indices. Remote Sens. 15. https://doi.org/10.3390/rs15092381.
Ratter, J.A., Richards, P.W., Argent, G., Gifford, D.R., Clapham, A.R., 1973. Observations on the vegetation of northeastern Mato Grosso: I. The woody vegetation types of the Xavantina-Cachimbo Expedition Area. Philos. Trans. R. Soc. Lond. Ser. B Biol. Sci. 266, 449–492. https://doi.org/10.1098/rstb.1973.0053.
Reiche, J., Mullissa, A., Slagter, B., Gou, Y., Tsendbazar, N.-E., Odongo-Braun, C., Vollrath, A., Weisse, M.J., Stolle, F., Pickens, A., Donchyts, G., Clinton, N., Gorelick, N., Herold, M., 2021. Forest disturbance alerts for the Congo Basin using Sentinel-1. Environ. Res. Lett. 16, 024005. https://doi.org/10.1088/1748-9326/abd0a8.
Reis, S.M., Lenza, E., Marimon, B.S., Gomes, L., Forsthofer, M., Morandi, P.S., Marimon Junior, B.H., Feldpausch, T.R., Elias, F., 2015. Post-fire dynamics of the woody vegetation of a savanna forest (Cerradão) in the Cerrado-Amazon transition zone. Acta Bot. Bras. 29, 408–416. https://doi.org/10.1590/0102-33062015abb0009.
Reis, S.M., de Oliveira, E.A., Elias, F., Gomes, L., Morandi, P.S., Marimon, B.S., Marimon Junior, B.H., das Neves, E.C., de Oliveira, B., Lenza, E., 2017. Resistance to fire and the resilience of the woody vegetation of the "Cerradão" in the "Cerrado"–Amazon transition zone. Braz. J. Bot 40, 193–201. https://doi.org/10.1007/s40415-016-0336-1.
Reis, S.M., Marimon, B.S., Marimon Junior, B.H., Morandi, P.S., de Oliveira, E.A., Elias, F., das Neves, E.C., de Oliveira, B., Nogueira, D.S., Umetsu, R.K., Feldpausch, T.R., Phillips, O.L., 2018. Climate and fragmentation affect forest structure at the southern border of Amazonia. Plant Ecol. Divers. 11, 13–25. https://doi.org/10.1080/17550874.2018.1455230.
Reygadas, Y., Spera, S., Galati, V., Salisbury, D.S., Silva, S., Novoa, S., 2021. Mapping forest disturbances across the southwestern Amazon: tradeoffs between open-source, Landsat-based algorithms. Environ. Res. Commun. 3, 091001. https://doi.org/10.1088/2515-7620/ac2210.
Ribeiro, A.F.S., Santos, L., Randerson, J.T., Uribe, M.R., Alencar, A.A.C., Macedo, M.N., Morton, D.C., Zscheischler, J., Silvestrini, R.A., Rattis, L., Seneviratne, S.I., Brando, P.M., 2024. The time since land-use transition drives changes in fire activity in the Amazon-Cerrado region. Commun. Earth Environ. 5, 96. https://doi.org/10.1038/s43247-024-01248-3.
Ribeiro, J.F., Walter, B.M.T., 2008. As principais fitofissionomias do bioma cerrado. In: Cerrado: Ecologia e Flora, pp. 151–212.
Ribeiro, J.M.P., Maculan, G., de Ávila, B.O., Morais, V.A., Hoeckesfeld, L., Secchi, L., de Andrade Guerra, J.B.S.O., 2025. Deforestation by production displacement: expansion of cropland and cattle ranching on Amazon Forest. Environ. Dev. Sustain. 1–32. https://doi.org/10.1007/s10668-024-05917-3.
Rodman, K.C., Andrus, R.A., Veblen, T.T., Hart, S.J., 2021. Disturbance detection in Landsat time series is influenced by tree mortality agent and severity, not by prior disturbance. Remote Sens. Environ. 254, 112244. https://doi.org/10.1016/j.rse.2020.112244.
Rodrigues, C.A., Zirondi, H.L., Fidelis, A., 2021. Fire frequency affects fire behavior in open savannas of the Cerrado. For. Ecol. Manag. 482, 118850. https://doi.org/10.1016/j.foreco.2020.118850.
Rosan, T.M., Sitch, S., Mercado, L.M., Heinrich, V., Friedlingstein, P., Aragão, L.E.O.C., 2022. Fragmentation-driven divergent trends in burned area in Amazonia and Cerrado. Front. For. Global Change 5. https://doi.org/10.3389/ffgc.2022.801408.
Ros-Tonen, M.A., Van Andel, T., Morsello, C., Otsuki, K., Rosendo, S., Scholz, I., 2008. Forest-related partnerships in Brazilian Amazonia: there is more to sustainable forest management than reduced impact logging. For. Ecol. Manag. 256, 1482–1497. https://doi.org/10.1016/j.foreco.2008.02.044.
Roy, D.P., Kovalskyy, V., Zhang, H.K., Vermote, E.F., Yan, L., Kumar, S.S., Egorov, A., 2016. Characterization of Landsat-7 to Landsat-8 reflective wavelength and

normalized difference vegetation index continuity. Remote Sens. Environ. 185, 57–70. https://doi.org/10.1016/j.rse.2015.12.024.
Rußwurm, M., Körner, M., 2020. Self-attention for raw optical satellite time series classification. ISPRS J. Photogramm. Remote Sens. 169, 421–435. https://doi.org/10.1016/j.isprsjprs.2020.06.006.
Salimans, T., Kingma, D.P., 2016. Weight normalization: a simple reparameterization to accelerate training of deep neural networks. Adv. Neural Inf. Proces. Syst., 29
Sano, E.E., 2019. Land use expansion in the Brazilian Cerrado. In: Hosono, A., Hamaguchi, N., Bojanic, A. (Eds.), Innovation with Spatial Impact: Sustainable Development of the Brazilian Cerrado. Springer, Singapore, pp. 137–162. https://doi.org/10.1007/978-981-13-6182-1_5.
Santana, N.C., Júnior, O.A. de C., Gomes, R.A.T., Fontes Guimarães, R., 2020. Comparison of post-fire patterns in Brazilian savanna and tropical forest from remote sensing time series. ISPRS Int. J. Geo Inf. 9, 659. https://doi.org/10.3390/ijgi9110659.
Santos, M.C. da R., Galvão, L.S., Korting, T.S., Rodigheri, G., 2025. Effects of precipitation and fire on land surface phenology in the Brazilian savannas (Cerrado). Remote Sens. 17. https://doi.org/10.3390/rs17122077.
Sawyer, D., 2008. Climate change, biofuels and eco-social impacts in the Brazilian Amazon and Cerrado. Philos. Trans. R. Soc. B Biol. Sci. 363, 1747–1752. https://doi.org/10.1098/rstb.2007.0030.
Schmidt, M.V.C., Ikpeng, Y.U., Kayabi, T., Sanches, R.A., Ono, K.Y., Adams, C., 2021. Indigenous knowledge and forest succession management in the Brazilian Amazon: contributions to reforestation of degraded areas. Front. For. Glob. Change 4. https://doi.org/10.3389/ffgc.2021.605925.
Schroeder, T.A., Wulder, M.A., Healey, S.P., Moisen, G.G., 2011. Mapping wildfire and clearcut harvest disturbances in boreal forests with Landsat time series data. Remote Sens. Environ. 115, 1421–1433. https://doi.org/10.1016/j.rse.2011.01.022.
Senf, C., Müller, J., Seidl, R., 2019. Post-disturbance recovery of forest cover and tree height differ with management in Central Europe. Landsc. Ecol. 34, 2837–2850. https://doi.org/10.1007/s10980-019-00921-9.
SERVIR-Amazonia, 2023. Running the LandTrendr GUI [WWW Document]. In: Barbados Geospatial Capacity Building Training. URL. https://servir-amazonia.github.io/barbados-training/time-series-change1/lt-tutorial-1.html (accessed 2.24.26).
Shimizu, K., Ota, T., Mizoue, N., Yoshida, S., 2019. A comprehensive evaluation of disturbance agent classification approaches: strengths of ensemble classification, multiple indices, spatio-temporal variables, and direct prediction. ISPRS J. Photogramm. Remote Sens. 158, 99–112. https://doi.org/10.1016/j.isprsjprs.2019.10.004.
da Silva Arruda, V.L., Alencar, A.A.C., de Carvalho Júnior, O.A., de Figueiredo Ribeiro, F., de Arruda, F.V., Conciani, D.E., da Silva, W.V., Shimbo, J.Z., 2024. Assessing four decades of fire behavior dynamics in the Cerrado biome (1985 to 2022). Fire Ecol. 20, 1–20. https://doi.org/10.1186/s42408-024-00298-4.
Silva, C.V.J., Aragão, L.E.O.C., Barlow, J., Espirito-Santo, F., Young, P.J., Anderson, L.O., Berenguer, E., Brasil, I., Foster Brown, I., Castro, B., Farias, R., Ferreira, J., França, F., Graça, P.M.L.A., Kirsten, L., Lopes, A.P., Salimon, C., Scaranello, M.A., Seixas, M., Souza, F.C., Xaud, H.A.M., 2018. Drought-induced Amazonian wildfires instigate a decadal-scale disruption of forest carbon dynamics. Philos. Trans. R. Soc. B 373, 20180043. https://doi.org/10.1098/rstb.2018.0043.
Silva Junior, C.H.L., Anderson, L.O., Silva, A.L., Almeida, C.T., Dalagnol, R., Pletsch, M. A.J.S., Penha, T.V., Paloschi, R.A., Aragão, L.E.O.C., 2019. Fire responses to the 2010 and 2015/2016 Amazonian droughts. Front. Earth Sci. 7. https://doi.org/10.3389/feart.2019.00097.
Silva Junior, C.H.L., Aragão, L.E.O.C., Anderson, L.O., Fonseca, M.G., Shimabukuro, Y.E., Vancutsem, C., Achard, F., Beuchle, R., Numata, I., Silva, C.A., Maeda, E.E., Longo, M., Saatchi, S.S., 2020. Persistent collapse of biomass in Amazonian forest edges following deforestation leads to unaccounted carbon losses. Sci. Adv. 6, eaaz8360. https://doi.org/10.1126/sciadv.aaz8360.
Silvério, D.V., Brando, P.M., Balch, J.K., Putz, F.E., Nepstad, D.C., Oliveira-Santos, C., Bustamante, M.M.C., 2013. Testing the Amazon savannization hypothesis: fire effects on invasion of a neotropical forest by native cerrado and exotic pasture grasses. Philos. Trans. R. Soc. Lond. Ser. B Biol. Sci. 368, 20120427. https://doi.org/10.1098/rstb.2012.0427.
Simoes, R., Camara, G., Queiroz, G., Souza, F., Andrade, P.R., Santos, L., Carvalho, A., Ferreira, K., 2021. Satellite image time series analysis for big Earth observation data. Remote Sens. 13. https://doi.org/10.3390/rs13132428.
de Souza, A.A., Galvão, L.S., Korting, T.S., Almeida, C.A., 2021. On a data-driven approach for detecting disturbance in the Brazilian savannas using time series of vegetation indices. Remote Sens. 13, 4959. https://doi.org/10.3390/rs13244959.
de Souza Mendes, F., Baron, D., Gerold, G., Liesenberg, V., Erasmi, S., 2019. Optical and SAR remote sensing synergism for mapping vegetation types in the endangered Cerrado/Amazon ecotone of Nova Mutum–Mato Grosso. Remote Sens. 11, 1161. https://doi.org/10.3390/rs11101161.
Souza-Alonso, P., Saiz, G., García, R.A., Pauchard, A., Ferreira, A., Merino, A., 2022. Post-fire ecological restoration in Latin American forest ecosystems: insights and lessons from the last two decades. For. Ecol. Manag. 509, 120083. https://doi.org/10.1016/j.foreco.2022.120083.
Spracklen, D.V., Garcia-Carreras, L., 2015. The impact of Amazonian deforestation on Amazon basin rainfall. Geophys. Res. Lett. 42, 9546–9552. https://doi.org/10.1002/2015GL066063.
Staver, A.C., Archibald, S., Levin, S.A., 2011. The global extent and determinants of savanna and forest as alternative biome states. Science 334, 230–232. https://doi.org/10.1126/science.1210465.
Torello-Raventos, M., Feldpausch, T.R., Veenendaal, E., Schrodt, F., Saiz, G., Domingues, T.F., Djagbletey, G., Ford, A., Kemp, J., Marimon, B.S., Hur Marimon Junior, B., Lenza, E., Ratter, J.A., Maracahipes, L., Sasaki, D., Sonké, B., Zapfack, L., Taedoumg, H., Villarroel, D., Schwarz, M., Quesada, C.A., Yoko Ishida, F., Nardoto, G.B., Affum-Baffoe, K., Arroyo, L., Bowman, M.J.S.D., Compaore, H., Davies, K., Diallo, A., Fyllas, N.M., Gilpin, M., Hien, F., Johnson, M., Killeen, T.J., Metcalfe, D., Miranda, H.S., Steininger, M., Thomson, J., Sykora, K., Mougin, E., Hiernaux, P., Bird, M.I., Grace, J., Lewis, S.L., Phillips, O.L., Lloyd, J., 2013. On the delineation of tropical vegetation types with an emphasis on forest/savanna transitions. Plant Ecol. Divers. 6, 101–137. https://doi.org/10.1080/17550874.2012.762812.
Tu, Y., Liao, K., Chen, Y., Jiao, H., Chen, G., 2024. Optimized parameters for detecting multiple forest disturbance and recovery events and spatiotemporal patterns in fast-regrowing southern China. Remote Sens. 16. https://doi.org/10.3390/rs16122240.
USDA Forest Service, 2023. Geospatial Technology and Applications Center (GTAC). U.S. Department of Agriculture Forest Service.
Vancutsem, C., Achard, F., Pekel, J.-F., Vieilledent, G., Carboni, S., Simonetti, D., Gallego, J., Aragão, L.E.O.C., Nasi, R., 2021. Long-term (1990–2019) monitoring of forest cover changes in the humid tropics. Sci. Adv. 7, eabe1603. https://doi.org/10.1126/sciadv.abe1603.
Vanpoucke, K., Heremans, S., Buls, E., Somers, B., 2024. Field-level classification of winter catch crops using Sentinel-2 time series: model comparison and transferability. Remote Sens. 16. https://doi.org/10.3390/rs16244620.
Verburg, R., Rodrigues Filho, S., Lindoso, D., Debortoli, N., Litre, G., Bursztyn, M., 2014. The impact of commodity price and conservation policy scenarios on deforestation and agricultural land use in a frontier area within the Amazon. Land Use Policy 37, 14–26. https://doi.org/10.1016/j.landusepol.2012.10.003.
Vieira, L.T.A., Azevedo, T.N., Castro, A.A.J.F., Martins, F.R., 2022. Reviewing the Cerrado's limits, flora distribution patterns, and conservation status for policy decisions. Land Use Policy 115, 106038. https://doi.org/10.1016/j.landusepol.2022.106038.
Vourlitis, G.L., Dalmagro, H.J., Pinto, O.B., Vieira, R.N., Malhado, C.R.R., de Arruda, P. H.Z., 2026. Rapid recovery of Brazilian tropical savanna woodlands (Cerrado *stricto sensu*) to prescribed burns. Trees For. People 23, 101129. https://doi.org/10.1016/j.tfp.2025.101129.
Wang, Y., Ziv, G., Adami, M., Mitchard, E., Batterman, S.A., Buermann, W., Schwantes Marimon, B., Marimon Junior, B.H., Matias Reis, S., Rodrigues, D., Galbraith, D., 2019. Mapping tropical disturbed forests using multi-decadal 30 m optical satellite imagery. Remote Sens. Environ. 221, 474–488. https://doi.org/10.1016/j.rse.2018.11.028.
Wearn, O.R., Reuman, D.C., Ewers, R.M., 2012. Extinction debt and windows of conservation opportunity in the Brazilian Amazon. Science 337, 228–232. https://doi.org/10.1126/science.1219013.
Wei-Jian, H., Yong-Tao, L., Yuan, H., 2021. Prediction of chaotic time series using hybrid neural network and attention mechanism. Acta Phys. Sin. 70.
White, J.C., Wulder, M.A., Hermosilla, T., Coops, N.C., Hobart, G.W., 2017. A nationwide annual characterization of 25 years of forest disturbance and recovery for Canada using Landsat time series. Remote Sens. Environ. 194, 303–321. https://doi.org/10.1016/j.rse.2017.03.035.
White, J.C., Saarinen, N., Kankare, V., Wulder, M.A., Hermosilla, T., Coops, N.C., Pickell, P.D., Holopainen, M., Hyyppä, J., Vastaranta, M., 2018. Confirmation of post-harvest spectral recovery from Landsat time series using measures of forest cover and height derived from airborne laser scanning data. Remote Sens. Environ. 216, 262–275. https://doi.org/10.1016/j.rse.2018.07.004.
Yin, F., Lewis, P.E., Gómez-Dans, J.L., 2022. Bayesian atmospheric correction over land: Sentinel-2/MSI and Landsat 8/OLI. Geosci. Model Dev. 15, 7933–7976. https://doi.org/10.5194/gmd-15-7933-2022.
Zaiatz, A.P.S.R., Zolin, C.A., Vendrusculo, L.G., Lopes, T.R., Paulino, J., 2018. Agricultural land use and cover change in the Cerrado/Amazon ecotone: a case study of the upper Teles Pires River basin. Acta Amaz 48, 168–177. https://doi.org/10.1590/1809-4392201701930.
Zhu, Z., Woodcock, C.E., 2012. Object-based cloud and cloud shadow detection in Landsat imagery. Remote Sens. Environ. 118, 83–94. https://doi.org/10.1016/j.rse.2011.10.028.